Synthesis and Antitumor Activities of Novel Mitochondria-Targeted Dihydroartemisinin Ether Derivatives

Cangcang Xu,[†] Linfan Xiao,[†] Peiyu Lin, Xiyue Yang, Xin Zou, Lingli Mu,* and Xiaoping Yang*

ACCESS | Metrics & More | Article Recommendations | Supporting Information

DHA

6.3 fold

Mitochondria-targeted moiety

ether linker with 8 carbons

D8-T (α+β)

IC_{50} T24 Cancer cell = 56.9 ± 3.2 nM
IC_{50} J82 Cancer cell = 61.8 ± 3.3 nM

Bax | Bcl-2

D8-T

Mitochondria

MMP → ROS → Cell apoptosis

ATP → Cell cycle arrest at G1 phase

Cyclin D1 | CDK6 | CDK4 | p21

Cell growth and proliferation
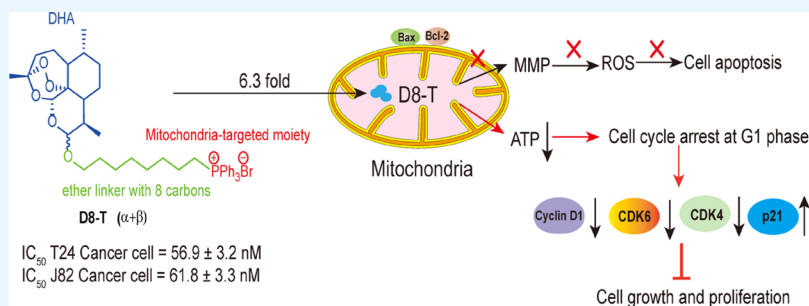
ABSTRACT: Ten novel mitochondria-targeted dihydroartemisinin ether derivatives were designed, synthesized, and evaluated for antitumor activity against five cancer cell lines in vitro. Profoundly, compound **D8-T** (IC_{50} = 56.9 nM) showed the most potent antiproliferative activity against the T24 cells with low cytotoxicity in normal human umbilical vein endothelial cells. High-performance liquid chromatography analysis confirmed that **D8-T** targeted mitochondria 6.3-fold higher than DHA. ATP content assay demonstrated that **D8-T** decreased the ATP level of bladder cancer cells. The effect of **D8-T** on cell apoptosis was determined by flow cytometry and western blot of Bax and Bcl-2. Surprisingly, the results indicated that **D8-T** did not induce bladder cancer cell apoptosis. In contrast, the cell cycle analysis and western blot of CDK4, CDK6, cyclin D1, and p21 demonstrated that the cancer cell cycle was arrested at the G1 phase after **D8-T** treatment. Furthermore, the consistent results were received by RNA-seq assay. These promising findings implied that **D8-T** could serve as a great candidate against bladder cancer for further investigation.

1. INTRODUCTION

Artemisinin (ART), a first-line antimalaria drug with a peroxide bridge in its structure, was extracted and separated from Compositae family member *Artemisia annua* L. (sweet worm-wood).[1−3] Dihydroartemisinin (DHA), the reduction product of ART, has better water solubility and stronger antimalarial activity than ART. DHA is the primary active metabolite of artesunate, artemether, and arteether as well.[4] Recent studies showed that DHA displays antitumor effects on various types of tumors, including lung cancer,[5,6] ovarian cancer,[7] prostate cancer,[8] and bladder cancer.[9] The antitumor mechanism of DHA includes inhibition of proliferation,[10] induction of apoptosis and ferroptosis,[5,11] and autophagy.[12] However, in our previous study, we found that DHA displayed antitumor activity in a relatively high dose at a micromolar level.[13−15] Furthermore, high dosage of DHA causes neurotoxicity, largely limiting its clinical antitumor application.[16,17] Thus, there is an urgent need to find novel DHA derivatives with higher antitumor activity to satisfy their clinical transformation.

Mitochondria are termed the powerhouses of the cells, producing energy in the form of ATP required by the cells. In addition to producing energy, mitochondria store calcium for cell signaling activities, generate reactive oxygen species (ROS), and mediate cell growth and death. Mitochondria dysfunctions can influence biosynthetic and cellular signal transduction pathways, transcription factors, and chromatin structure to shift the cell from a quiescent, differentiated state to an actively proliferative one.[18] Recent studies showed that the trans-membrane potential of mitochondria in cancer cells exceeded the potential of healthy cell organelles.[19] The lipophilic cationic molecules could selectively accumulate in the tumor cell mitochondria and modulate their functions. Based on this principle, various delocalized lipophilic cations containing rhodamine-123,[20] F16,[21] dequalinium,[22] berberine,[23] and triphenylphosphonium (TPP)[15] cations have been successfully used for the targeted delivery of natural active molecules into the mitochondria. Curcumin,[24] glycyrrhetinic acid,[25] and betulinic acid[21,26] have been linked with TPP cations or F16 cations to obtain novel mitochondria-targeted small molecules with higher antitumor activity and better safety.
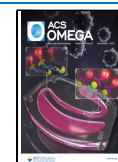
In our previous study, TPP-containing mitochondria-targeted ART ester derivatives with higher antitumor activity than DHA were discovered,[15] indicating that the introduction of mitochondria-targeted moiety TPP$^+$ may be beneficial to the antitumor activity of DHA. Furthermore, Zhang et al. reported that antitumor activity of mitochondria-targeted bisNHC gold(I) complexes, using DHA ether derivatives as a building block, reached at a nanomolar level of IC$_{50}$.[27] Based on these recent findings, a series of novel derivatives with mitochondria-targeted moiety TPP$^+$ and building block DHA ether were designed and synthesized in this study. Furthermore, the antitumor activities of these compounds were evaluated, and the underlying mechanisms of the selected compound were explored.

2. RESULTS AND DISCUSSION

2.1. Chemistry. The syntheses of compounds **D3~D12** were the etherification of DHA and the corresponding bromoalcohol using boron trifluoride etherate as a Lewis acid catalyst in dichloromethane as shown in Scheme 1. The target compounds **D3-T~D12-T** were synthesized by reacting compounds **D3~D12** respectively with triphenylphosphine in the presence of potassium carbonate as a base under refluxing conditions as shown in Scheme 1.

Scheme 1. Synthesis Route of Compounds D3-T to D12-T[a]
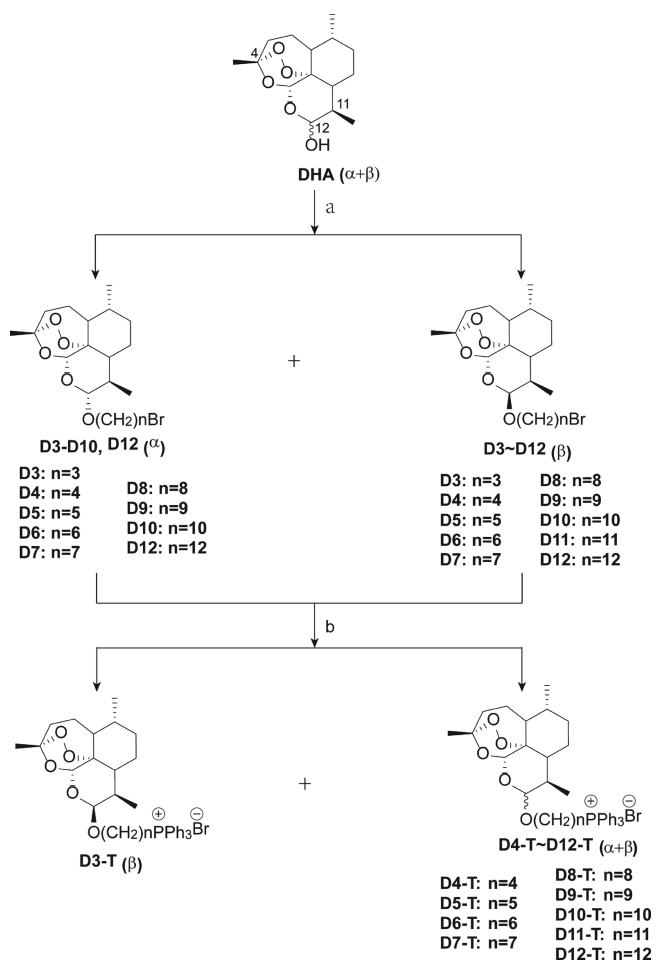
[a]Reagents and conditions: a. bromoalcohol, BF$_3$·Et$_2$O, dry CH$_2$Cl$_2$, rt, 12 h, and N$_2$; b. PPh$_3$, K$_2$CO$_3$, acetonitrile, reflux, 24 h, and N$_2$.

The structures of 10 novel DHA derivatives and intermediates were confirmed by proton nuclear magnetic resonance (^{1}H NMR), carbon nuclear magnetic resonance (^{13}C NMR), and high-resolution-electrospray ionization mass spectrometry (HR-ESIMS). For **D11** and **D3-T**, the 12β-isomer was exclusively attained, evident from the coupling constants ($J \approx 3-4$ Hz) of H-11 and H-12 in ^{1}H NMR.[28] For **D3~D10** and **D12**, the 12β-isomer and 12α-isomer ($J \approx 5$ Hz or $J > 9$ Hz) were respectively attained. For **D4-T~D12-T**, the mixtures containing the 12β-isomer and 12α-isomer were obtained. Additionally, the ^{13}C NMR spectrum of C-4 at about δ_C 104 ppm in all compounds suggested the presence of the intact peroxide.[29] The appearance of aromatic peaks in the ^{1}H NMR spectrum at about δ_H 7.43−7.88 ppm (15H) confirmed the presence of phenyl groups. Similarly, in ^{13}C NMR spectra, new aromatic carbon peaks appeared at about δ_C 135.02/134.99 (d, $J_{C,P}$ = 3.0 Hz, Ph-C), 133.70/133.68 (d, $J_{C,P}$ = 9.0 Hz, Ph-C), 132.08 (d, $J_{C,P}$ = 9.0 Hz, Ph-C), 131.97 (d, J = 3.0 Hz, Ph-C), 130.51/130.48 (d, J = 12.0 Hz, Ph-C), 128.51 (d, J = 12.0 Hz, Ph-C), and 118.44/118.40 (d, J = 85.5 Hz, Ph-C) ppm, confirming the presence of phenyl groups.

2.2. In Vitro Antitumor Activity Assay. The antitumor activities of all compounds were evaluated against selected five cancer cell lines (human ovarian cancer OVCAR3 and SKOV3 cells, non-small cell lung cancer A549 cells, and human bladder cancer J82 and T24 cells) and were assessed for toxicities against human umbilical vein endothelial (HUVEC) cells using MTT assay. The IC$_{50}$ values of all compounds are shown in Table 1. In the OVCAR3 cell line, **D8-T**, **D9-T**, and **D10-T** exhibited potent antitumor activity with IC$_{50}$ values ranging from 90.7 to 99.8 nM. In the SKOV3 cell line, **D5-T**, **D7-T**, **D8-T**, **D10-T**, and **D12-T** exhibited potent antitumor activity with IC$_{50}$ values ranging from 65.3 to 98.0 nM. In the J82 cell line, **D8-T**, **D9-T**, **D10-T**, **D11-T**, and **D12-T** exhibited potent antitumor activity with IC$_{50}$ values ranging from 61.8 to 91.9 nM. In the T24 cell line, **D8-T** and **D7-T** displayed potent antitumor activity with IC$_{50}$ values of 56.9 and 60.5 nM, respectively. In the A549 cell line, **D8-T** and **D7-T** showed potent antitumor activity with IC$_{50}$ values of 126.3 and 138.0 nM, respectively. Among these compounds, **D8-T** had potent antitumor activity against all tested cell lines with greatest selectivity (Selectivity index = IC$_{50(\text{HUVEC})}$/IC$_{50(\text{T24})}$ = 4.4) against the T24 cell line. Compared with DHA,[14] the antitumor activity of D8-T against T24 cells increased 1256.6 times. Therefore, **D8-T** was selected for further pharmacological mechanism studies in T24 and J82 cells.

2.3. T24 Mitochondria Uptake Assay. To verify the targeting effect on mitochondria of **D8-T**, the uptake of **D8-T** and DHA in the mitochondria was evaluated in T24 cells. Mitochondria were extracted from T24 cells after 4 h of treatment with 10 μM **D8-T** and DHA, respectively, and then the contents of **D8-T** and DHA were analyzed by high-performance liquid chromatography (HPLC). As shown in Figure 1A−C, the uptake of **D8-T** was elevated 6.3-fold compared with DHA (59.5 vs 9.5 nmol/mg protein), indicating that the targeting capacity of **D8-T** to mitochondria was greatly enhanced by introducing the TPP$^+$ moiety.

Mitochondria generate ATP to satisfy the energy needs of the cells.[30] The production of ATP in J82 and T24 cells after **D8-T** treatment with different concentrations was detected by the ATP detection kit. As shown in Figure 1D, the ATP contents of J82 and T24 cells significantly declined after **D8-T** treatment in 25, 50, and 100 nM compared with the control group, indicating

Table 1. Antitumor Activity of Compounds D3-T~D12-T against OVCAR3, SKOV3, J82, T24, A549, and HUVEC Cell Lines

compounds	IC$_{50}$ (nM)						SI = IC$_{50(HUVEC)}$/IC$_{50(T24)}$
	OVCAR3	SKOV3	J82	T24	A549	HUVEC	
D3-T	133.7 ± 20.0	150.3 ± 28.6	229.1 ± 11.5	259.0 ± 27.7	178.9 ± 5.7	433.9 ± 20.6	1.67
D4-T	243.1 ± 16.7	192.3 ± 30.7	188.5 ± 7.1	357.1 ± 52.1	223.0 ± 11.0	495.5 ± 38.7	1.39
D5-T	176.8 ± 14.4	95.0 ± 6.3	178.9 ± 11.5	347.6 ± 13.2	279.0 ± 16.1	409.8 ± 25.1	1.18
D6-T	129.1 ± 27.8	104.8 ± 8.1	170.4 ± 10.6	156.0 ± 9.4	186.8 ± 10.8	322.4 ± 10.2	2.07
D7-T	102.5 ± 5.5	$\mathbf{98.0 \pm 8.6}$	114.7 ± 17.6	$\mathbf{60.5 \pm 3.4}$	$\mathbf{138.0 \pm 17.5}$	161.7 ± 4.1	2.67
D8-T	$\mathbf{99.8 \pm 5.6}$	$\mathbf{74.7 \pm 10.2}$	$\mathbf{61.8 \pm 3.3}$	$\mathbf{56.9 \pm 3.2}$	$\mathbf{126.3 \pm 21.4}$	251.8 ± 31.1	**4.42**
D9-T	$\mathbf{95.6 \pm 1.5}$	103.0 ± 5.3	91.9 ± 5.0	115.7 ± 4.4	224.2 ± 21.0	258.4 ± 23.7	2.23
D10-T	$\mathbf{90.7 \pm 14.5}$	$\mathbf{65.3 \pm 8.1}$	86.8 ± 7.3	107.4 ± 12.9	166.6 ± 19.2	329.6 ± 20.9	3.07
D11-T	116.7 ± 17.3	118.5 ± 8.7	$\mathbf{87.4 \pm 8.1}$	153.1 ± 14.5	184.8 ± 21.1	148.3 ± 9.3	0.97
D12-T	100.8 ± 6.3	77.3 ± 19.7	82.1 ± 11.2	116.4 ± 11.8	189.3 ± 18.9	76.1 ± 7.3	0.65
DHA	87.2 ± 1.2^a	NT	146.2 ± 10.3^a	71.5 ± 5.24^b	NT	180.1 ± 7.2^a	
cisplatin	13.1 ± 0.9^a	NT	6.9 ± 0.8^a	NT	NT	NT	

^{a}The data are from ref 15 and the unit was μM. ^{b}The data are from ref 14 and the unit was μM. NT: no test.
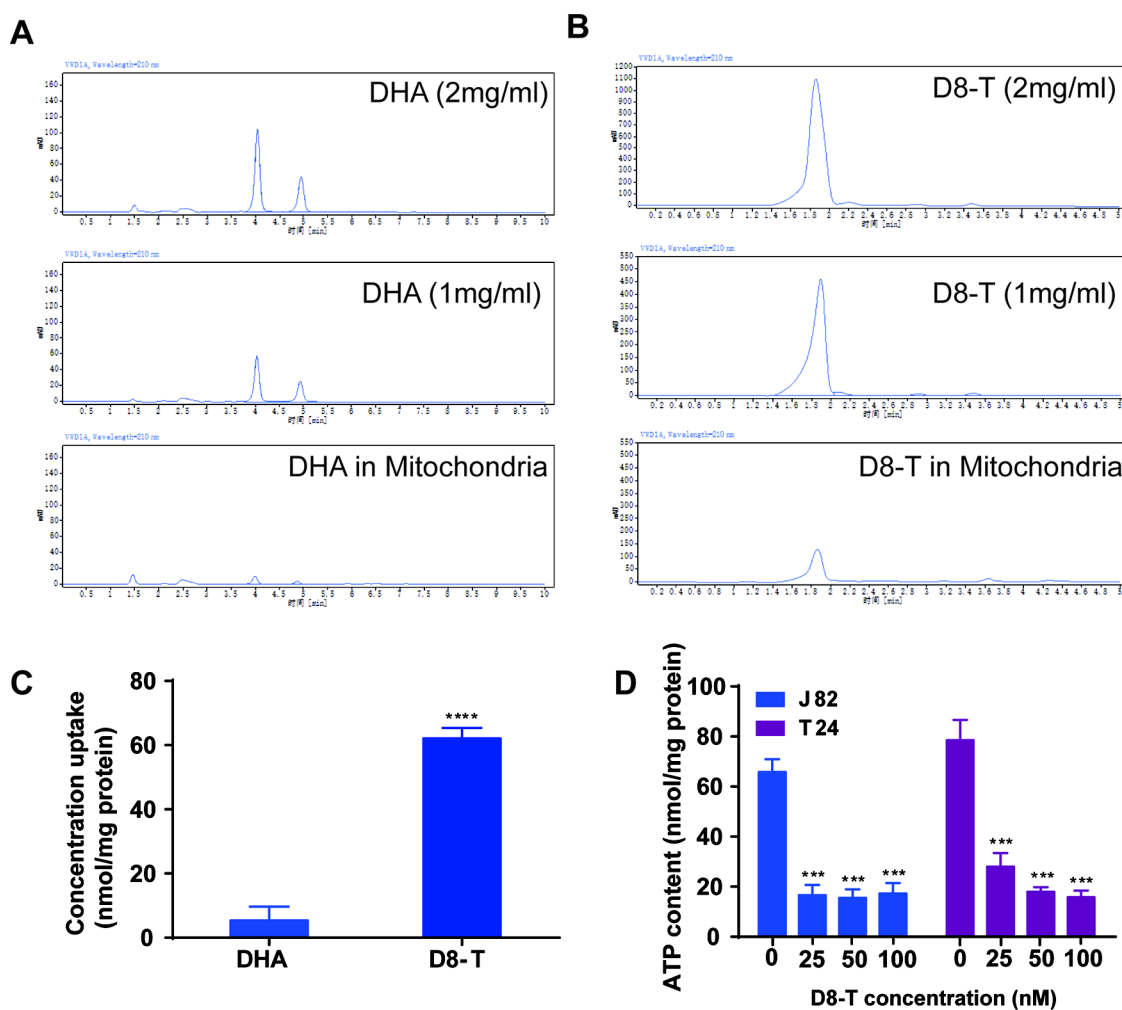

Figure 1. Cellular uptake of DHA and D8-T in the mitochondria of T24 cells. (A and B) Uptake by mitochondria of DHA and D8-T was analyzed with HPLC. (C) Quantitative data of DHA and D8-T in mitochondria after normalization to the protein content. The results are the mean $\pm$ SD of three independent experiments. ****$P < 0.0001$, vs DHA. (D) ATP content after D8-T treatment (0, 25, 50, 100 nM) in J82 and T24 cells. The results are the mean $\pm$ SD of three independent experiments. ***$P < 0.001$, vs control.

that **D8-T** interfered with mitochondrial function by reducing the ATP level.

2.4. D8-T Inhibited Colony Formation and Cell Migration in Bladder Cancer Cells. Because **D8-T** showed excellent inhibition of proliferative activity using MTT assay, its

ability to inhibit cellular colony formation and cell migration were further evaluated through colony formation assay and cellular scratch assay, respectively. As shown in Figure 2A−D, **D8-T** exhibited stronger inhibitory activity on colony formation and cell migration in J82 and T24 cell lines than DHA at the
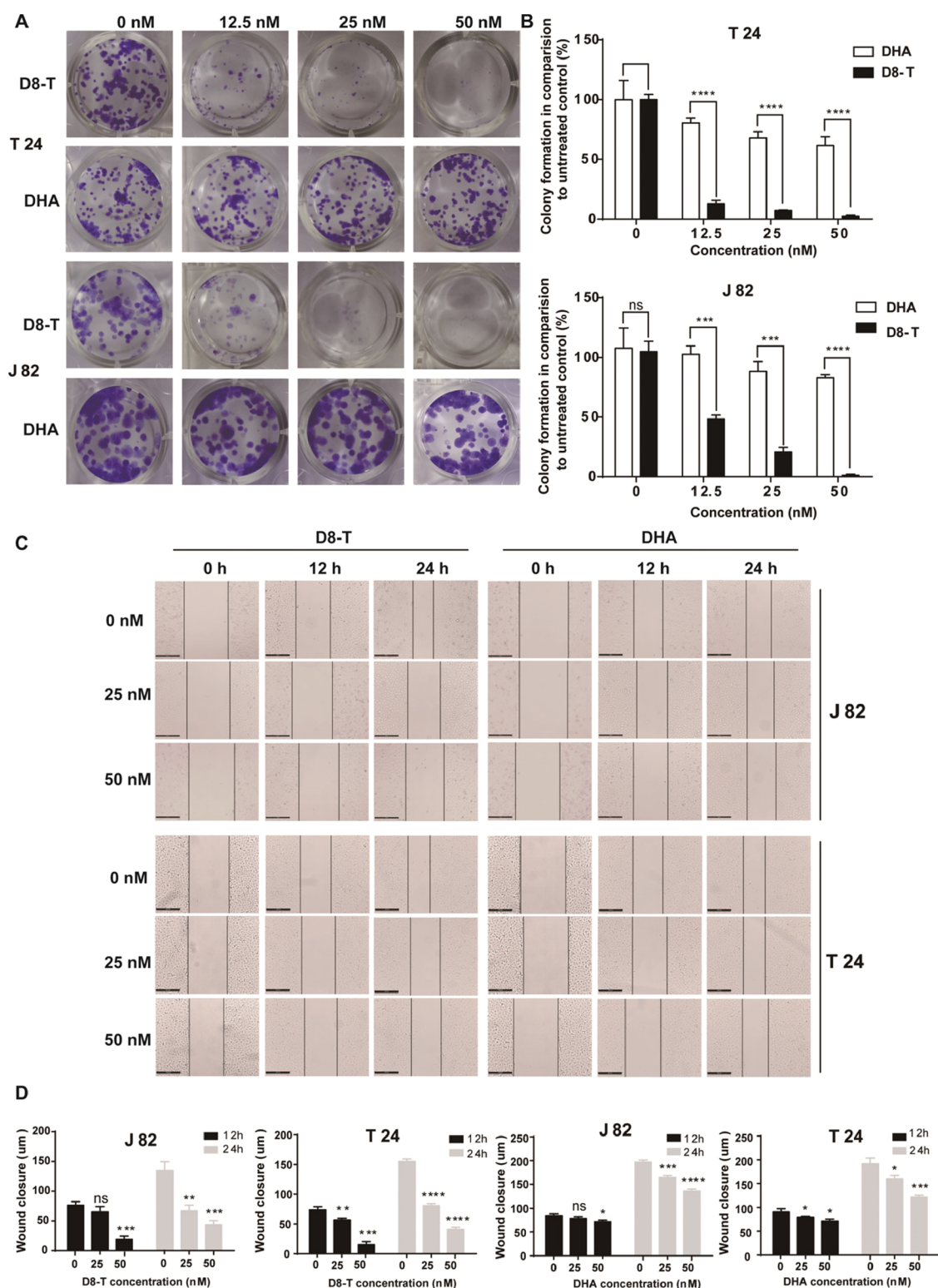
Figure 2. Inhibitory effect of DHA and D8-T on colony formation and cell migration in J82 and T24 cells. (A) Colony formation of T24 and J82 cells after the treatment of DHA and D8-T. (B) Quantitative data of colony formation. (C) Gap of scratch areas after D8-T and DHA treatment or without D8-T and DHA treatment for 0, 12, or 24 h. Scale bar: 200 μm. (D) Average wound closure distance was obtained using Image J software. The results were showed as the average of three independent experiments. ns: no significance, *$P < 0.05$, **$P < 0.01$, ***$P < 0.001$, and ****$P < 0.0001$, vs control.

same concentration. These results demonstrated that **D8-T** had a stronger inhibitory effect than DHA in J82 and T24 cells.

2.5. D8-T Significantly Inhibited Bladder Cancer Cell Proliferation. Uncontrollable proliferation is a major feature of malignant tumors, and inhibition of tumor cell proliferation is of

great significance for cancer treatment. Therefore, EdU assay was used to further determine the antiproliferation activity of **D8-T** in bladder cancer cells. As shown in Figure 3A,B, treatment with **D8-T** significantly decreased the proliferation of J82 and T24 cells in a dose-dependent manner. PCNA, also
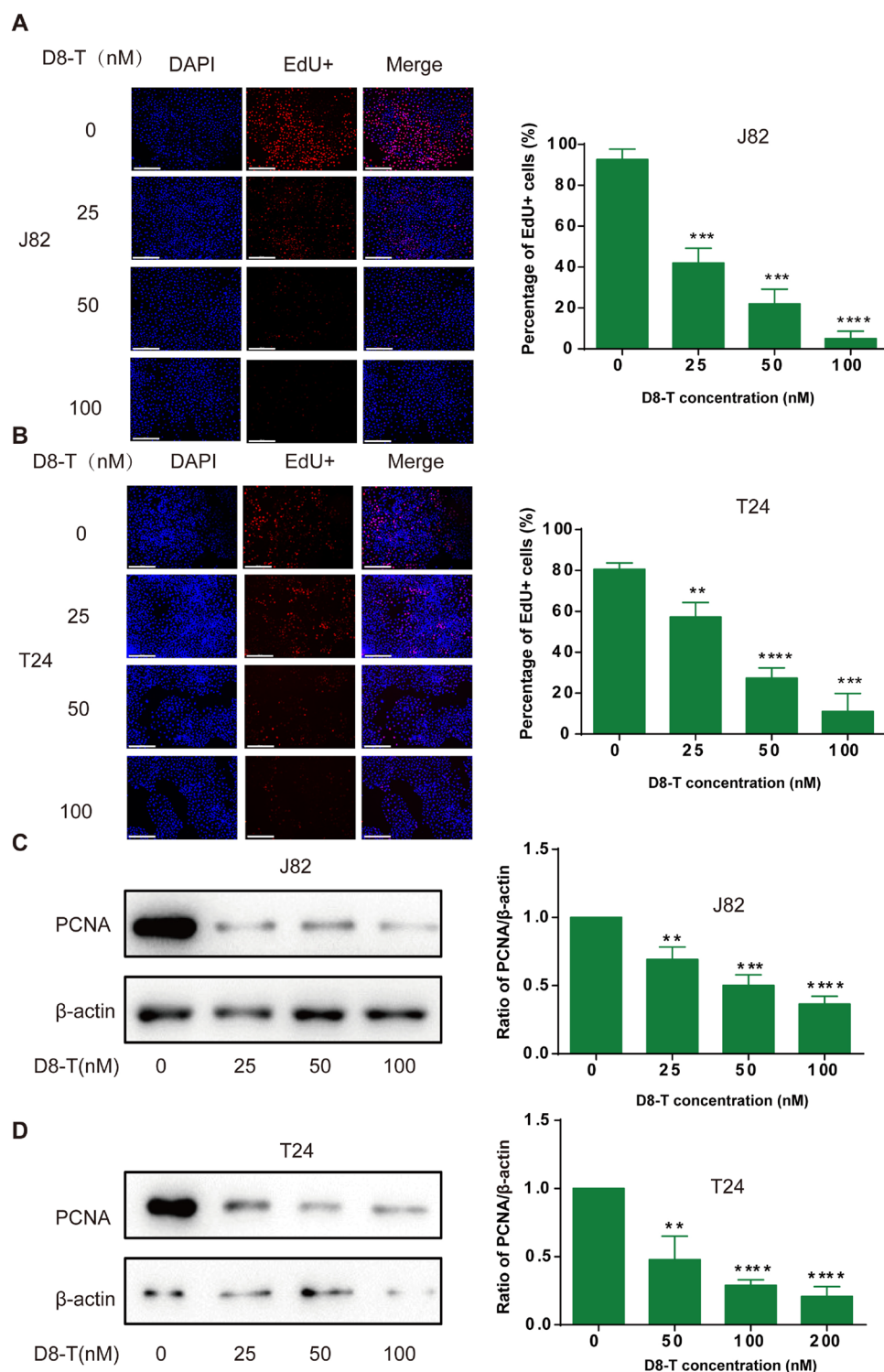
Figure 3. D8-T inhibits the proliferation of J82 and T24 cells. (A and B) J82 and T24 cells were treated with D8-T, and proliferation was assessed by the EdU assay. Scale bar: 200 μm. (C and D) Effect of D8-T on the expression of PCNA in J82 and T24 cells was determined by western blot. β-Actin was used as an endogenous reference. The results are the mean ± SD of three independent experiments. ** $P < 0.01$, *** $P < 0.001$, and **** $P < 0.0001$, vs control.

known as proliferating cell nuclear antigen, is another key protein marker in cell proliferation.[31] The results of western blot showed that **D8-T** treatment significantly decreased the protein expression of PCNA (Figure 3C,D). Collectively, the data confirmed that **D8-T** strongly suppresses the proliferation of J82 and T24 cells.

2.6. D8-T Did Not Induce Bladder Cancer Cell Apoptosis.
Generally, mitochondria play an important role in regulating cell apoptosis. To confirm the effect on cell apoptosis of **D8-T** in bladder cancer cells, the cell apoptosis-related assay of **D8-T** was performed. The data from the flow cytometry analysis of J82 cells treated with or without **D8-T** for 48 h are presented in Figure 4A−C. Surprisingly, treatment of J82 cells
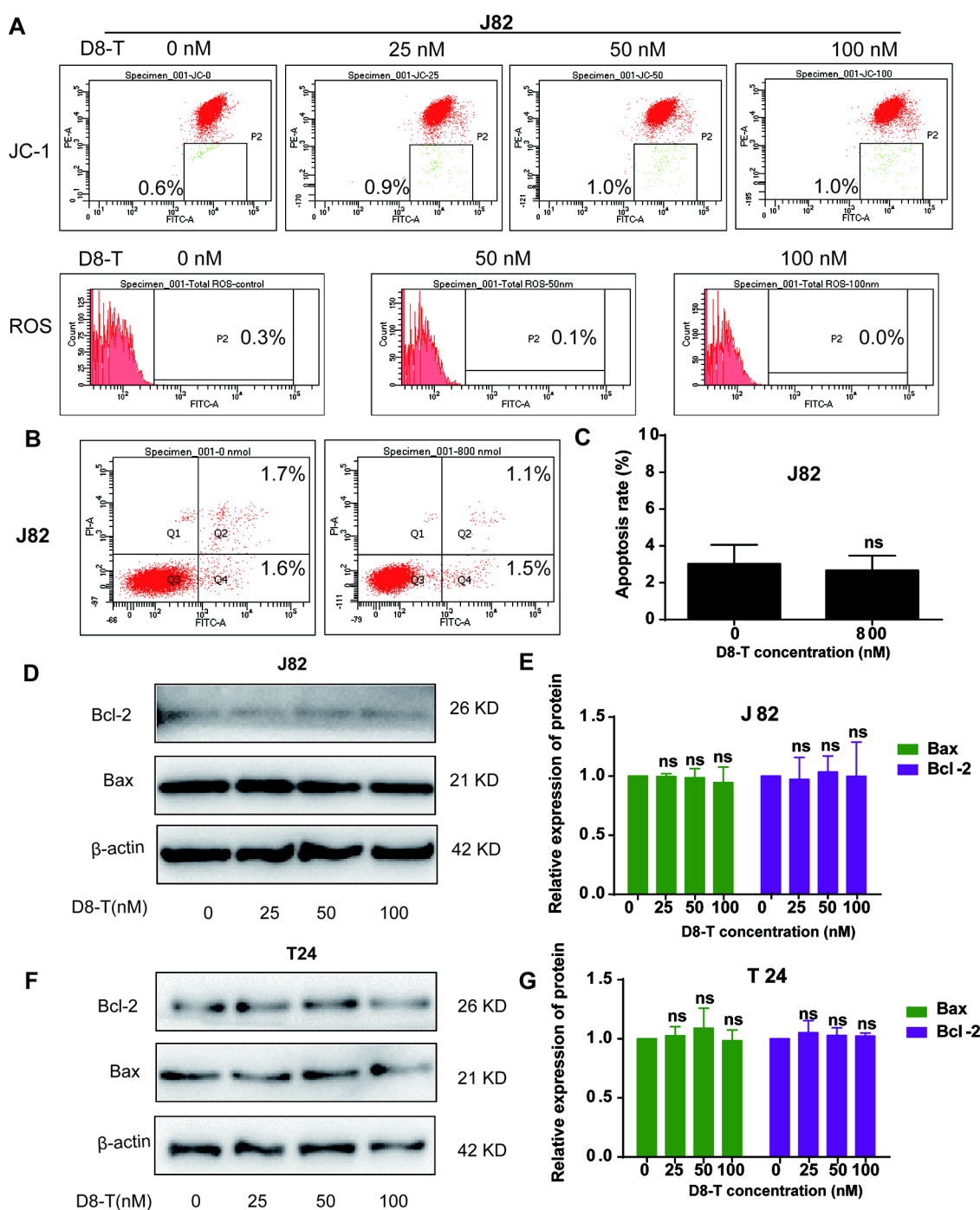
Figure 4. D8-T did not induce the bladder cancer cells apoptosis. (A) J82 cells were treated with D8-T for 48 h and then analyzed by flow cytometry after JC-1 staining and DCFH-DA treatment. (B and C) J82 cells were treated with D8-T for 48 h; apoptosis of J82 cells was evaluated by flow cytometry. (D−G) Effects of D8-T on the expression of apoptosis-related proteins (Bax and Bcl-2) were examined by western blot analysis. The results are the mean ± SD of three independent experiments. ns, vs control.

with **D8-T** did not lead to the decrease of mitochondrial membrane potential (MMP). Meanwhile, compared with those in the untreated cells, the increase of the apoptotic population and ROS production was not observed either in treated cells. Moreover, the results of western blot showed that **D8-T** treatment did neither increase the expression level of Bax nor decrease the expression level of Bcl-2 (Figure 4D−G). Collectively, the data confirmed that **D8-T** suppresses the bladder cancer cell proliferation independent of cell apoptosis.

2.7. D8-T Induced Bladder Cancer Cell Cycle Arrested at the G1 Phase. Mitochondrial dynamics is also intimately linked to cell cycle progression.[32,33] It is well known that ATP generated by mitochondria induced the cell cycle progression, and ATP was necessary for cells to enter the S phase in the cell cycle.[34,35] To prove whether the cell cycle entering the S phase was affected by the **D8-T**-induced decrease of the ATP level, flow cytometric analysis of J82 and T24 cells stained by propidium iodide (PI) was performed after treatment with different concentrations of **D8-T** (0, 25, 50, and 100 nM) for 48
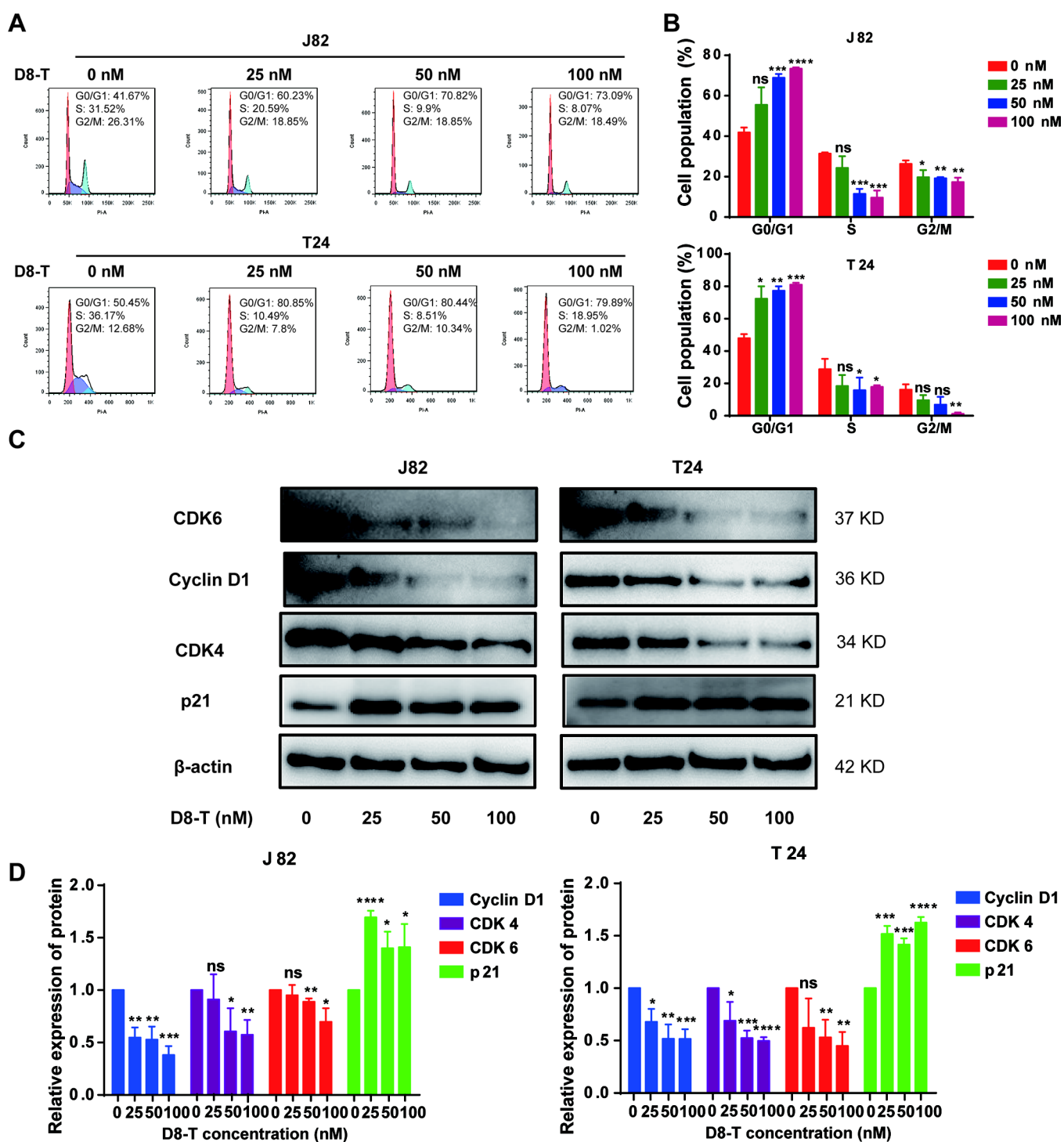
Figure 5. D8-T-induced cell cycle arrest at the G1 phase. (A and B) Effects of D8-T on cell cycle progression of J82 and T24 cells were detected by flow cytometry. (C and D) Effects of D8-T on the expression of cell cycle-related proteins (cyclin D1, CDK6, CDK4, and p21) were examined by western blot analysis. The results are the mean ± SD of three independent experiments. *$P < 0.05$, **$P < 0.01$, ***$P < 0.001$, and ****$P < 0.0001$, vs control.

h. As expected, compared with the control group, in the increased concentration of **D8-T**, the proportion of G1 phase cells increased from 41.67 to 73.09% in J82 cells and from 50.45 to 79.89% in T24 cells, while S and G2/M phase cells decreased from 57.83 to 26.56% in J82 cells and from 48.85 to 19.97% in T24 cells after **D8-T** treatment, compared with the control group (Figure 5A,B). The results indicated that **D8-T** induced cell cycle G1 phase arrest with inhibition of cell cycle entrance to S and G2/M phases. Moreover, the results of western blot

showed that **D8-T** treatment decreased the expression levels of cyclin D1, CDK6, and CDK4 and increased the expression level of p21 (Figure 5C,D). Cyclin D1 plays dual roles in proliferation and in cell apoptosis.[36] The phenomenon that **D8-T** arrested cell cycle at the G1 phase but did not induce cell apoptosis may be due to regulation of cyclin D1. Taken together, the results indicated that **D8-T** inhibited bladder cancer cell proliferation by arresting the cell cycle at the G1 phase.
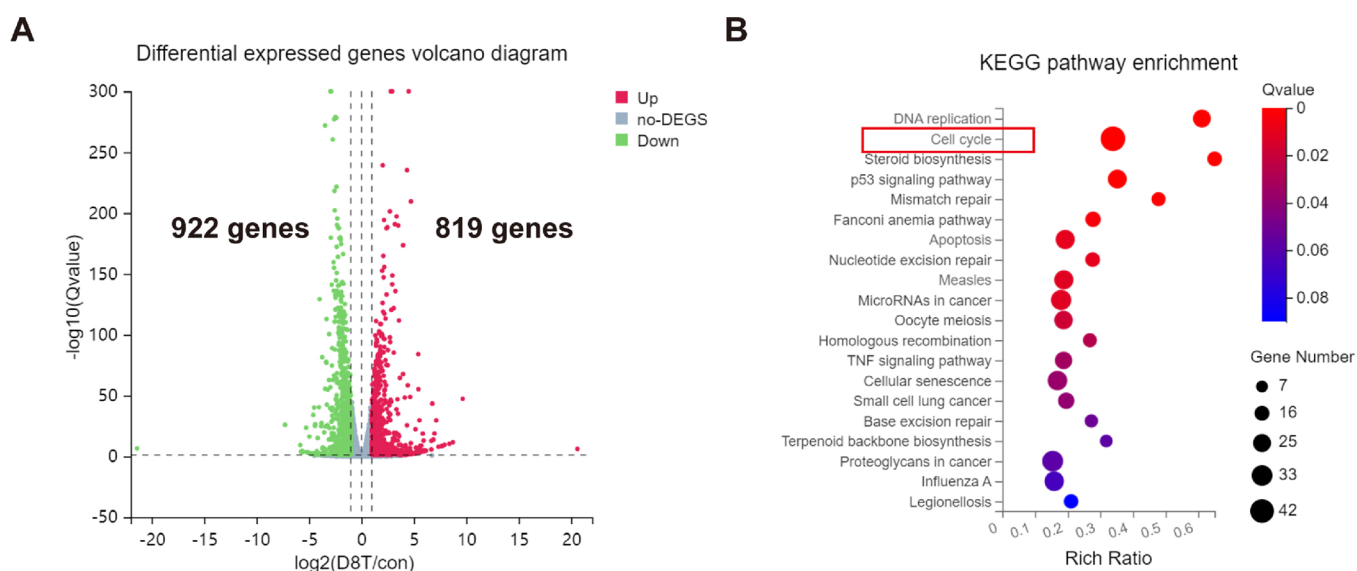
A

B

Figure 6. (A) Volcano diagram of the D8-T-regulated genes. (B) Scatter plots for KEGG pathway analysis showing upregulation or downregulation of genes following 48 h treatment of T24 cells with 200 nM D8-T in comparison with the control group. The horizontal axis represents the rich ratio of the DEGs in each term. The vertical axis shows the description of each term.

2.8. RNA-seq Analysis Identified the Effect of D8-T on the Cell Cycle. The RNA-seq analysis using T24 cells was performed to identify the signaling pathway influenced by **D8-T**. The differential gene volcano diagram was generated to visualize the distribution of differentially expressed genes (DEGs) between control and **D8-T**-treated T24 cells with |$\log_2 FC$| $\geq$ 1 and $Qvalue \leq 0.05$. The results showed that 819 genes were upregulated and 922 genes were downregulated (Figure 6A). The KEGG pathway enrichment analysis of these genes revealed changes in expression of genes linked to DNA replication, cell cycle, steroid biosynthesis, and so on. The 42 most DEGs were observed linked to the cell cycle (Figure 6B), which was consistent with the above results.

3. CONCLUSIONS

In conclusion, 10 novel mitochondria-targeted DHA ether derivatives were synthesized and evaluated for their antitumor activity against selected five human cancer cell lines. These novel derivatives displayed much stronger antitumor activity than DHA with IC_{50} at the nanomolar level. **D8-T** was the highest efficient and lowest toxic antitumor molecule against T24 cells. **D8-T** has a strong mitochondria-targeted capability and decreased the ATP level of bladder cancer cells. The mechanistic study revealed that **D8-T** arrested cell cycle at the G1 phase but did not induce cell apoptosis. RNA-seq analysis obtained consistent results. In general, **D8-T** should be further intensively investigated for a more detailed mechanism and the development of novel antibladder cancer drugs in future.

4. EXPERIMENTAL SECTION

4.1. Materials and Measurements. ^{1}H NMR and ^{13}C NMR spectra were obtained in chloroform-*d* on a Bruker DRX 600 spectrophotometer using TMS as the internal standard. Mass spectra were acquired on a 6540 Q-TOF (Agilent). Column chromatography was performed using silica gel (Qingdao Marine Chemical Co., Ltd., China). The purity of target compounds was determined using an Agilent 1260 HPLC system which was equipped with an autoinjector, a binary pump, and a diode array detector. The chromatographic separation was

achieved on a Diamonsil-C18 column (250 × 4.6 mm, 5 μm). The mobile phase system consisted of A (water) and B (acetonitrile). The linear gradient program was set as follows: time (min)/% of mobile phase B: 0/5; 60/90 for **D3-T~D6-T** (0/30; 60/95 for **D7-T~D12-T**). The detection wavelength and flow rate were 210 nm and 1 mL/min, respectively.

All commercially available reagents were used without further purification unless otherwise stated. The progress of the reactions was monitored by analytical thin-layer chromatography (TLC) performed on homemade HSGF254 precoated silica gel plates. Visualization was performed by UV or development using vanillin solution in sulfuric acid and ethanol (4/1 v/v). Yields were reported after chromatographic purification.

4.2. Chemical Synthesis of Target Compounds. *4.2.1. General Procedure for the Synthesis of Compounds D3~D12.* The compounds **D3** to **D12** were obtained by one-step etherification reaction. To a three-necked flask (500 mL) that contained a solution of DHA (1 equiv) and bromoalcohol (1.03 equiv) in dry CH_2Cl_2 were slowly added four drops of $BF_3 \cdot Et_2O$ (Scheme 1). The resulting mixture was stirred at rt for 12 h under N_2. Then the saturated $NaHCO_3$ solution was added and extracted with CH_2Cl_2, dried over anhydrous sodium carbonate, and purified using column chromatography to obtain the target compounds.

4.2.1.1. Compound D3. Yield: 12.93%. Pale yellow oil. β-Isomer; ^{1}H NMR (600 MHz, Chloroform-d) δ 5.42 (s, 1H), 4.80 (d, J = 3.5 Hz, 1H), 4.00 (ddd, J = 10.0, 6.6, 5.1 Hz, 1H), 3.49 (q, J = 6.4 Hz, 3H), 2.64 (qdd, J = 7.5, 4.7, 3.5 Hz, 1H), 2.37 (ddd, J = 14.7, 13.5, 4.0 Hz, 1H), 2.15−1.99 (m, 3H), 1.88 (dddd, J = 13.7, 6.8, 4.0, 3.1 Hz, 1H), 1.80−1.69 (m, 2H), 1.63 (dq, J = 13.2, 3.4 Hz, 1H), 1.55−1.44 (m, 2H), 1.44 (s, 3H), 1.33 (qp, J = 9.7, 3.7, 3.3 Hz, 1H), 1.28−1.21 (m, 2H), 0.95 (d, J = 6.4 Hz, 3H), 0.90 (d, J = 7.4 Hz, 3H). ^{13}C NMR (150 MHz, Chloroform-d) δ 104.12, 102.11, 87.93, 81.05, 65.70, 52.58, 44.39, 37.46, 36.43, 34.64, 32.55, 30.90, 30.61, 26.20, 24.67, 24.52, 20.37, 12.98. HRESI-MS m/z: $C_{18}H_{29}BrO_5$ 427.1085 (M + Na)+:429.1067 (M + 2 + Na)+ = 1:1.

α-Isomer; ^{1}H NMR (600 MHz, Chloroform-d) δ 5.34 (s, 1H), 4.44 (d, J = 9.2 Hz, 1H), 4.07 (dt, J = 10.1, 5.1 Hz, 1H), 3.64–3.47 (m, 3H), 2.46–2.32 (m, 2H), 2.21 (ddq, J = 16.7, 8.5, 5.6 Hz, 1H), 2.09–1.96 (m, 2H), 1.88 (ddt, J = 13.6, 6.8, 3.5 Hz, 1H), 1.76 (dq, J = 13.6, 3.7 Hz, 1H), 1.72–1.66 (m, 1H), 1.57–1.46 (m, 2H), 1.43 (s, 3H), 1.36–1.26 (m, 3H), 1.04–0.98 (m, 1H), 0.96 (dd, J = 6.8, 4.7 Hz, 3H), 0.89 (d, J = 7.1 Hz, 3H). ^{13}C NMR (150 MHz, Chloroform-d) δ 104.29, 100.42, 91.21, 80.35, 66.45, 51.65, 45.33, 37.39, 36.32, 34.24, 32.78, 32.67, 30.83, 26.06, 24.72, 22.21, 20.29, 12.58. HRESI-MS m/z: $C_{18}H_{29}BrO_5$ 427.1086 (M + Na)$^+$:429.1064 (M + 2 + Na)$^+$ = 1:1.

4.2.1.2. Compound D4. Yield: 10.9%. Pale yellow oil. β-Isomer; ^{1}H NMR (600 MHz, Chloroform-d) δ 5.37 (s, 1H), 4.77 (d, J = 3.5 Hz, 1H), 3.88 (dt, J = 9.8, 6.2 Hz, 1H), 3.50–3.35 (m, 3H), 2.69–2.57 (m, 1H), 2.36 (ddd, J = 14.7, 13.5, 4.0 Hz, 1H), 2.03 (ddd, J = 14.6, 5.0, 3.0 Hz, 1H), 1.97–1.84 (m, 3H), 1.79–1.68 (m, 4H), 1.63 (dq, J = 13.3, 3.4 Hz, 1H), 1.54–1.44 (m, 2H), 1.43 (s, 3H), 1.33 (ttd, J = 12.4, 6.3, 4.0 Hz, 1H), 1.28–1.15 (m, 2H), 0.95 (d, J = 6.4 Hz, 3H), 0.90 (d, J = 7.4 Hz, 3H). ^{13}C NMR (150 MHz, Chloroform-d) δ 104.10, 102.01, 87.92, 81.10, 67.44, 52.58, 44.42, 37.49, 36.44, 34.64, 33.63, 30.90, 29.82, 28.34, 26.21, 24.68, 24.50, 20.37, 13.04. HRESI-MS m/z: $C_{19}H_{31}BrO_5$ 441.1235 (M + Na)$^+$:443.2 (M + 2 + Na)$^+$ = 1:1.

α-Isomer; ^{1}H NMR (600 MHz, Chloroform-d) δ 5.44 (s, 1H), 4.96 (d, J = 5.2 Hz, 1H), 3.91 (dt, J = 9.8, 6.3 Hz, 1H), 3.51 (dt, J = 9.9, 6.4 Hz, 1H), 3.45 (t, J = 6.8 Hz, 2H), 2.30 (td, J = 14.0, 3.9 Hz, 1H), 2.02 (ddd, J = 14.5, 4.8, 3.0 Hz, 1H), 1.97 (dq, J = 9.7, 7.0 Hz, 2H), 1.90 (ddq, J = 13.5, 6.6, 3.5 Hz, 1H), 1.76 (p, J = 6.9 Hz, 2H), 1.72–1.61 (m, 3H), 1.55–1.47 (m, 2H), 1.47–1.42 (m, 2H), 1.42 (s, 3H), 1.18 (d, J = 7.2 Hz, 3H), 0.99 (td, J = 12.3, 11.7, 4.1 Hz, 1H), 0.94 (d, J = 5.9 Hz, 3H), 0.93–0.86 (m, 1H). ^{13}C NMR (150 MHz, Chloroform-d) δ 103.01, 102.78, 89.17, 81.67, 67.77, 51.86, 46.55, 39.89, 37.32, 36.53, 34.42, 33.71, 31.64, 29.74, 28.34, 25.98, 24.69, 20.07, 19.51. HRESI-MS m/z: $C_{19}H_{31}BrO_5$ 441.1239 (M + Na)$^+$:443.1355 (M + 2 + Na)$^+$ = 1:1.

4.2.1.3. Compound D5. Yield: 19.72%. Pale yellow oil. β-Isomer; ^{1}H NMR (600 MHz, Chloroform-d) δ 5.39 (s, 1H), 4.77 (d, J = 3.4 Hz, 1H), 3.85 (dt, J = 9.8, 6.3 Hz, 1H), 3.47–3.32 (m, 3H), 2.68–2.52 (m, 1H), 2.42–2.30 (m, 1H), 2.03 (ddd, J = 14.6, 5.0, 3.0 Hz, 1H), 1.91–1.84 (m, 3H), 1.81 (dd, J = 13.9, 3.6 Hz, 1H), 1.75 (tt, J = 14.3, 3.8 Hz, 1H), 1.66–1.55 (m, 4H), 1.54–1.45 (m, 4H), 1.43 (s, 3H), 1.42–1.28 (m, 3H), 1.28–1.16 (m, 1H), 0.95 (d, J = 6.4 Hz, 3H), 0.90 (d, J = 7.8 Hz 3H). ^{13}C NMR (150 MHz, Chloroform-d) δ 104.08, 102.01, 87.93, 81.15, 68.03, 52.59, 44.46, 37.47, 36.45, 34.68, 33.84, 32.43, 30.94, 28.84, 26.23, 24.98, 24.69, 24.50, 20.37, 13.05. ESI-MS m/z: $C_{20}H_{33}BrO_5$ 455.2 (M + Na)$^+$:457.2 (M + 2 + Na)$^+$ = 1:1.

α-Isomer; ^{1}H NMR (600 MHz, Chloroform-d) δ 5.44 (s, 1H), 4.95 (d, J = 5.0 Hz, 1H), 3.87 (dt, J = 9.8, 6.5 Hz, 1H), 3.48 (dt, J = 9.8, 6.5 Hz, 1H), 3.41 (t, J = 6.8 Hz, 2H), 2.30 (ddd, J = 14.6, 13.4, 3.9 Hz, 1H), 2.01 (ddd, J = 14.6, 4.8, 3.1 Hz, 1H), 1.89 (ddt, J = 13.9, 9.7, 5.3 Hz, 3H), 1.71 (qd, J = 13.4, 3.4 Hz, 2H), 1.63 (ddt, J = 12.0, 8.2, 4.8 Hz, 4H), 1.57 (dt, J = 13.3, 3.5 Hz, 2H), 1.54–1.49 (m, 3H), 1.41 (s, 3H), 1.18 (d, J = 7.3 Hz, 3H), 1.00–0.96 (m, 1H), 0.94 (d, J = 6.1 Hz, 3H), 0.90–0.85 (m, 1H). ^{13}C NMR (150 MHz, Chloroform-d) δ 103.04, 102.80, 89.10, 81.66, 68.40, 51.89, 46.52, 39.82, 37.30, 36.53, 34.44, 33.78, 32.54, 31.61, 28.83, 25.98, 24.92, 24.69, 20.07, 19.54. HRESI-MS m/z: $C_{20}H_{33}BrO_5$ 455.1396 (M + Na)$^+$:457.1379 (M + 2 + Na)$^+$ = 1:1.

4.2.1.4. Compound D6. Yield: 13.10%. Pale yellow oil. β-Isomer; ^{1}H NMR (600 MHz, Chloroform-d) δ 5.38 (s, 1H),

4.77 (d, J = 3.5 Hz, 1H), 3.83 (dt, J = 9.7, 6.5 Hz, 1H), 3.40 (t, J = 6.8 Hz, 2H), 3.36 (dd, J = 9.7, 6.4 Hz, 1H), 2.61 (qt, J = 7.4, 4.1 Hz, 1H), 2.40–2.32 (m, 1H), 2.03 (ddd, J = 14.6, 5.0, 3.0 Hz, 1H), 1.90–1.83 (m, 3H), 1.80 (dd, J = 13.7, 3.6 Hz, 1H), 1.75 (tq, J = 12.0, 3.9 Hz, 1H), 1.66–1.59 (m, 1H), 1.58 (d, J = 4.2 Hz, 2H), 1.56–1.45 (m, 4H), 1.44 (s, 3H), 1.42–1.28 (m, 4H), 1.24–1.16 (m, 1H), 0.95 (d, J = 6.3 Hz, 3H), 0.90 (d, J = 7.3 Hz, 3H). ^{13}C NMR (150 MHz, Chloroform-d) δ 104.07, 101.99, 87.92, 81.15, 68.24, 52.61, 44.48, 37.51, 36.46, 34.68, 33.80, 32.73, 30.95, 29.49, 27.89, 26.24, 25.46, 24.70, 24.49, 20.39, 13.05. HRESI-MS m/z: $C_{21}H_{35}BrO_5$ 464.2001 (M + NH$_4$)$^+$:466.1985 (M + 2 + NH$_4$)$^+$ = 1:1.

α-Isomer; ^{1}H NMR (600 MHz, Chloroform-d) δ 5.33 (s, 1H), 4.41 (d, J = 9.2 Hz, 1H), 3.97 (dt, J = 9.6, 6.3 Hz, 1H), 3.47–3.35 (m, 3H), 2.49–2.28 (m, 2H), 2.02 (ddd, J = 14.6, 5.0, 3.0 Hz, 1H), 1.87 (h, J = 6.8 Hz, 3H), 1.76 (dq, J = 13.5, 3.8 Hz, 1H), 1.66 (dddd, J = 33.0, 15.3, 7.8, 4.7 Hz, 2H), 1.57–1.45 (m, 4H), 1.44 (s, 4H), 1.42–1.27 (m, 5H), 1.01 (td, J = 12.7, 12.2, 3.2 Hz, 1H), 0.95 (d, J = 6.3 Hz, 3H), 0.88 (d, J = 7.1 Hz, 3H). ^{13}C NMR (150 MHz, Chloroform-d) δ 104.25, 100.12, 91.21, 80.35, 68.86, 51.69, 45.35, 37.39, 36.35, 34.27, 33.94, 32.75, 32.64, 29.37, 27.93, 26.08, 25.21, 24.72, 22.22, 20.30, 12.65. HRESI-MS m/z: $C_{21}H_{35}BrO_5$ 464.2003 (M + NH$_4$)$^+$:466.1987 (M + 2 + NH$_4$)$^+$ = 1:1.

4.2.1.5. Compound D7. Yield: 13.29%. Pale yellow oil. β-Isomer; ^{1}H NMR (600 MHz, Chloroform-d) δ 5.38 (s, 1H), 4.77 (dd, J = 3.5, 1.0 Hz, 1H), 3.82 (dt, J = 9.6, 6.6 Hz, 1H), 3.42–3.30 (m, 3H), 2.67–2.51 (m, 1H), 2.40–2.32 (m, 1H), 2.07–1.99 (m, 1H), 1.90–1.71 (m, 5H), 1.63 (dq, J = 13.1, 3.3 Hz, 1H), 1.58–1.44 (m, 5H), 1.44 (s, 3H), 1.42–1.40 (m, 1H), 1.39–1.29 (m, 6H), 1.24–1.17 (m, 1H), 0.95 (d, J = 6.3 Hz, 3H), 0.90 (d, J = 7.4 Hz, 3H). ^{13}C NMR (150 MHz, Chloroform-d) δ 104.06, 101.97, 87.91, 81.16, 68.32, 52.61, 44.50, 37.51, 36.46, 34.68, 33.95, 32.74, 30.95, 29.55, 28.47, 28.13, 26.24, 26.08, 24.70, 24.49, 20.40, 13.05. HRESI-MS m/z: $C_{22}H_{37}BrO_5$ 483.1724 (M + Na)$^+$: 485.1708 (M + 2 + Na)$^+$ = 1:1.

α-Isomer; ^{1}H NMR (600 MHz, Chloroform-d) δ 5.33 (s, 1H), 4.41 (d, J = 9.2 Hz, 1H), 4.04–3.88 (m, 1H), 3.45–3.29 (m, 3H), 2.46–2.33 (m, 2H), 2.02 (ddd, J = 14.6, 5.0, 3.0 Hz, 1H), 1.86 (tt, J = 14.5, 7.0 Hz, 3H), 1.76 (dq, J = 13.6, 3.8 Hz, 1H), 1.68 (dq, J = 13.3, 3.4 Hz, 1H), 1.60–1.45 (m, 4H), 1.44 (s, 3H), 1.42–1.27 (m, 9H), 1.04–0.97 (m, 1H), 0.95 (d, J = 6.3 Hz, 3H), 0.88 (d, J = 7.1 Hz, 3H). ^{13}C NMR (150 MHz, Chloroform-d) δ 104.25, 100.12, 91.21, 80.36, 69.02, 51.69, 45.35, 37.39, 36.35, 34.27, 34.01, 32.76, 32.64, 29.45, 28.54, 28.12, 26.08, 25.83, 24.73, 22.23, 20.30, 12.65. HRESI-MS m/z: $C_{22}H_{37}BrO_5$ 483.1715 (M + Na)$^+$:485.1699 (M + 2 + Na)$^+$ = 1:1.

4.2.1.6. Compound D8. Yield: 19.07%. Pale yellow oil. β-Isomer; ^{1}H NMR (600 MHz, Chloroform-d) δ 5.38 (s, 1H), 4.76 (d, J = 3.5 Hz, 1H), 3.83 (ddt, J = 22.6, 9.7, 6.6 Hz, 1H), 3.39 (td, J = 6.9, 1.7 Hz, 2H), 3.35 (dt, J = 9.7, 6.5 Hz, 1H), 2.60 (qt, J = 7.4, 4.0 Hz, 1H), 2.36 (td, J = 14.0, 4.0 Hz, 1H), 2.02 (ddd, J = 14.7, 5.2, 3.2 Hz, 1H), 1.84 (ddd, J = 14.4, 8.2, 5.5 Hz, 3H), 1.81–1.67 (m, 2H), 1.64 (t, J = 3.6 Hz, 1H), 1.61–1.51 (m, 3H), 1.51–1.44 (m, 2H), 1.43 (s, 3H), 1.32 (dq, J = 8.7, 5.6, 4.5 Hz, 9H), 1.18 (d, J = 7.2 Hz, 1H), 0.95 (d, J = 6.3 Hz, 3H), 0.89 (d, J = 7.3 Hz, 3H). ^{13}C NMR (150 MHz, Chloroform-d) δ 104.04, 101.95, 87.91, 81.16, 68.39, 52.61, 44.50, 37.50, 36.46, 34.70, 33.98, 32.80, 30.95, 29.62, 29.13, 28.72, 28.09, 26.24, 26.15, 24.70, 24.48, 20.40, 13.05. HRESI-MS m/z: $C_{23}H_{39}BrO_5$ 492.2317 (M + NH$_4$)$^+$:494.2294 (M + 2+ NH$_4$)$^+$ = 1:1.

α-Isomer; ^{1}H NMR (600 MHz, Chloroform-d) δ 5.32 (s, 1H), 4.41 (d, J = 9.2 Hz, 1H), 4.02−3.89 (m, 1H), 3.40 (t, J = 6.9 Hz, 3H), 2.48−2.31 (m, 2H), 2.01 (ddd, J = 14.6, 5.0, 3.0 Hz, 1H), 1.91−1.81 (m, 3H), 1.75 (dq, J = 13.6, 3.9 Hz, 1H), 1.71−1.64 (m, 2H), 1.63−1.45 (m, 5H), 1.43 (s, 3H), 1.42−1.36 (m, 2H), 1.31 (dd, J = 5.8, 3.3 Hz, 5H), 1.27 (d, J = 6.9 Hz, 1H), 1.00 (td, J = 12.7, 12.3, 3.6 Hz, 1H), 0.95 (d, J = 6.2 Hz, 3H), 0.93−0.89 (m, 1H), 0.87 (d, J = 7.1 Hz, 3H). ^{13}C NMR (150 MHz, Chloroform-d) δ 104.23, 100.10, 91.20, 80.35, 69.09, 51.69, 45.35, 37.38, 36.35, 34.27, 34.04, 33.99, 32.81, 32.76, 29.50, 29.19, 28.70, 28.12, 25.90, 24.72, 22.22, 20.30, 12.64. HRESI-MS m/z: $C_{23}H_{39}BrO_5$ 492.2321 (M + NH$_4$)$^+$:494.2304 (M + 2 + NH$_4$)$^+$ = 1:1.

4.2.1.7. Compound D9. Yield: 15.14%. Pale yellow oil. *β*-Isomer; ^{1}H NMR (600 MHz, Chloroform-d) δ 5.39 (s, 1H), 4.77 (d, J = 3.5 Hz, 1H), 3.82 (dt, J = 9.6, 6.6 Hz, 1H), 3.49−3.33 (m, 3H), 2.61 (qdd, J = 7.4, 4.6, 3.5 Hz, 1H), 2.41−2.25 (m, 1H), 2.03 (ddd, J = 14.6, 5.0, 3.0 Hz, 1H), 1.92−1.77 (m, 4H), 1.74 (dq, J = 14.3, 4.0 Hz, 1H), 1.63 (dq, J = 13.1, 3.4 Hz, 1H), 1.57−1.45 (m, 4H), 1.44 (s, 3H), 1.42 (d, J = 9.8 Hz, 2H), 1.38−1.27 (m, 10H), 1.24−1.17 (m, 1H), 0.95 (d, J = 6.3 Hz, 3H), 0.89 (d, J = 7.4 Hz, 3H). ^{13}C NMR (150 MHz, Chloroform-d) δ 104.05, 101.95, 87.91, 81.17, 68.41, 52.62, 44.51, 37.50, 36.47, 34.70, 34.02, 32.84, 30.96, 29.64, 29.40, 29.22, 28.71, 28.18, 26.25, 26.20, 24.71, 24.47, 20.40, 13.05. HRESI-MS m/z: $C_{24}H_{41}BrO_5$ 511.2019 (M + Na)$^+$:513.1964 (M + 2 + Na)$^+$ = 1:1.

α-Isomer; ^{1}H NMR (600 MHz, Chloroform-d) δ 5.33 (s, 1H), 4.41 (d, J = 9.2 Hz, 1H), 3.95 (ddd, J = 9.6, 7.0, 5.8 Hz, 1H), 3.47−3.31 (m, 3H), 2.49−2.30 (m, 2H), 2.06−1.99 (m, 1H), 1.95−1.87 (m, 1H), 1.87−1.81 (m, 4H), 1.77 (tq, J = 13.6, 3.8 Hz, 1H), 1.68 (dq, J = 13.4, 3.4 Hz, 1H), 1.58−1.46 (m, 4H), 1.44 (s, 3H), 1.41 (q, J = 6.2, 5.4 Hz, 3H), 1.31−1.29 (m, 6H), 1.22−1.14 (m, 1H), 1.08−0.98 (m, 2H), 0.95 (d, J = 6.3 Hz, 3H), 0.88 (d, J = 7.2 Hz, 3H). ^{13}C NMR (150 MHz, Chloroform-d) δ 104.24, 100.10, 91.20, 80.35, 69.14, 51.69, 45.35, 37.39, 36.35, 34.27, 34.06, 32.84, 32.65, 29.53, 29.37, 29.29, 28.71, 28.16, 26.08, 25.95, 24.73, 22.23, 20.30, 12.64. HRESI-MS m/z: $C_{24}H_{41}BrO_5$ 511.2025 (M + Na)$^+$:513.2137 (M + 2 + Na)$^+$ = 1:1.

4.2.1.8. Compound D10. Yield: 6.77%. Pale yellow oil. *β*-Isomer; ^{1}H NMR (600 MHz, Chloroform-d) δ 5.41 (s, 1H), 4.80 (d, J = 3.6 Hz, 1H), 3.86 (ddt, J = 21.0, 9.6, 6.6 Hz, 1H), 3.52−3.36 (m, 3H), 2.63 (qdd, J = 7.4, 4.6, 3.5 Hz, 1H), 2.36 (dddd, J = 37.8, 14.6, 13.5, 3.9 Hz, 1H), 2.05 (dtd, J = 14.1, 5.4, 3.1 Hz, 1H), 1.95−1.80 (m, 4H), 1.80−1.69 (m, 1H), 1.65 (dp, J = 12.8, 2.9 Hz, 1H), 1.60−1.47 (m, 4H), 1.46 (d, J = 9.2 Hz, 3H), 1.43 (d, J = 8.9 Hz, 1H), 1.32 (d, J = 9.8 Hz, 12H), 1.27−1.18 (m, 2H), 0.98 (d, J = 6.2 Hz, 3H), 0.92 (d, J = 7.2 Hz, 3H). ^{13}C NMR (150 MHz, Chloroform-d) δ 104.04, 101.94, 87.91, 81.17, 68.42, 52.62, 44.51, 37.50, 36.47, 34.71, 34.04, 32.84, 30.96, 29.65, 29.49, 29.37, 29.28, 28.77, 28.19, 26.25, 26.22, 24.71, 24.47, 20.40, 13.05. ESI-MS m/z: $C_{25}H_{43}BrO_5$ 525.4 (M + Na)$^+$:527.4 (M + 2 + Na)$^+$ = 1:1.

α-Isomer; ^{1}H NMR (600 MHz, Chloroform-d) δ 5.33 (s, 1H), 4.41 (d, J = 9.2 Hz, 1H), 3.95 (ddd, J = 9.5, 7.1, 5.8 Hz, 1H), 3.47−3.27 (m, 3H), 2.46−2.29 (m, 2H), 2.02 (ddd, J = 14.5, 4.9, 3.0 Hz, 1H), 1.91−1.81 (m, 3H), 1.76 (dq, J = 13.5, 3.7 Hz, 1H), 1.68 (dq, J = 13.4, 3.4 Hz, 1H), 1.59−1.46 (m, 4H), 1.44 (s, 3H), 1.43−1.39 (m, 2H), 1.37−1.26 (m, 13H), 1.10 (s, 1H), 1.05−0.98 (m, 1H), 0.95 (d, J = 6.3 Hz, 3H), 0.88 (d, J = 7.8 Hz, 3H). ^{13}C NMR (150 MHz, Chloroform-d) δ 104.24, 100.10, 91.20, 80.36, 69.18, 51.69, 45.36, 37.39, 36.36, 34.28,

34.08, 32.85, 32.65, 29.71, 29.55, 29.46, 29.37, 28.75, 28.18, 26.08, 25.98, 24.73, 22.23, 20.30, 12.64. HRESI-MS m/z: $C_{25}H_{43}BrO_5$ 520.2621 (M + NH$_4$)$^+$:522.261 (M + 2 + NH$_4$)$^+$ = 1:1.

4.2.1.9. Compound D11. Yield: 12.14%. Pale yellow oil. *β*-Isomer; ^{1}H NMR (600 MHz, Chloroform-d) δ 5.38 (s, 1H), 4.77 (d, J = 3.5 Hz, 1H), 3.81 (dt, J = 9.6, 6.6 Hz, 1H), 3.42−3.32 (m, 3H), 2.68−2.56 (m, 1H), 2.36 (ddd, J = 14.6, 13.5, 4.0 Hz, 1H), 2.03 (ddd, J = 14.6, 5.0, 3.0 Hz, 1H), 1.92−1.80 (m, 4H), 1.73 (dq, J = 14.4, 3.9 Hz, 1H), 1.64−1.59 (m, 1H), 1.58−1.45 (m, 4H), 1.43 (s, 3H), 1.42−1.39 (m, 2H), 1.35−1.23 (m, 15H), 0.95 (d, J = 6.3 Hz, 3H), 0.89 (d, J = 7.4 Hz, 3H). ^{13}C NMR (150 MHz, Chloroform-d) δ 104.05, 101.94, 87.91, 81.18, 68.44, 52.61, 44.51, 37.49, 36.47, 34.70, 34.06, 32.84, 30.96, 29.71, 29.65, 29.56, 29.47, 29.44, 29.31, 28.79, 28.19, 26.24, 24.70, 24.47, 20.40, 13.05. HRESI-MS m/z: $C_{26}H_{45}BrO_5$ 539.2347 (M + Na)$^+$:541.2331 (M + 2 + Na)$^+$ = 1:1.

4.2.1.10. Compound D12. Yield: 13.12%. Pale yellow oil. *β*-Isomer; ^{1}H NMR (600 MHz, Chloroform-d) δ 5.39 (s, 1H), 4.77 (d, J = 2.5 Hz, 1H), 3.82 (dt, J = 9.6, 6.6 Hz, 1H), 3.40 (t, J = 6.9 Hz, 2H), 3.36 (dt, J = 9.7, 6.4 Hz, 1H), 2.65−2.55 (m, 1H), 2.37 (ddd, J = 14.6, 13.5, 4.0 Hz, 1H), 2.03 (ddd, J = 14.6, 5.0, 3.0 Hz, 1H), 1.92−1.78 (m, 4H), 1.74 (dq, J = 14.2, 3.8 Hz, 1H), 1.62 (dq, J = 13.2, 3.4 Hz, 1H), 1.56−1.44 (m, 4H), 1.44 (s, 3H), 1.43−1.39 (m, 2H), 1.36−1.24 (m, 17H), 0.95 (d, J = 6.4 Hz, 3H), 0.90 (d, J = 7.4 Hz, 3H). ^{13}C NMR (150 MHz, Chloroform-d) δ 104.04, 101.94, 87.92, 81.18, 68.45, 52.62, 44.52, 37.49, 36.47, 34.71, 34.07, 32.85, 30.97, 29.66, 29.60, 29.55 (×2), 29.46, 29.33, 28.79, 28.19, 26.25 (×2), 24.71, 24.47, 20.40, 13.05. HRESI-MS m/z: $C_{27}H_{47}BrO_5$ 548.2937 (M + NH$_4$)$^+$:550.2921 (M + 2 + NH$_4$)$^+$ = 1:1.

α-Isomer; ^{1}H NMR (600 MHz, Chloroform-d) δ 5.33 (s, 1H), 4.41 (d, J = 9.2 Hz, 1H), 3.98−3.85 (m, 1H), 3.44−3.30 (m, 3H), 2.45−2.31 (m, 2H), 2.02 (ddd, J = 14.5, 4.9, 2.9 Hz, 1H), 1.90−1.82 (m, 3H), 1.76 (dq, J = 13.6, 3.7 Hz, 1H), 1.68 (dq, J = 13.4, 3.5 Hz, 1H), 1.60−1.46 (m, 5H), 1.44 (s, 3H), 1.43−1.39 (m, 2H), 1.38−1.27 (m, 13H), 1.24−1.09 (m, 2H), 1.03−0.97 (m, 1H), 0.95 (d, J = 6.3 Hz, 3H), 0.91 (ddd, J = 9.3, 5.3, 2.6 Hz, 1H), 0.88 (d, J = 7.2 Hz, 3H). ^{13}C NMR (150 MHz, Chloroform-d) δ 104.24, 100.10, 91.20, 80.36, 69.22, 51.69, 45.36, 37.39, 36.36, 34.28, 34.09, 32.86, 32.65, 29.57 (×2), 29.54, 29.52, 29.44, 29.42, 28.78, 28.19, 26.08, 26.00, 24.73, 22.23, 20.30, 12.64. HRESI-MS m/z: $C_{27}H_{47}BrO_5$ 548.2935 (M + NH$_4$)$^+$:550.2923 (M + 2 + NH$_4$)$^+$ = 1:1.

4.2.2. General Procedure for the Synthesis of Target Compounds D3-T∼D12-T. To a round-bottom flask, a solution of **D3** to **D12** (1 equiv), triphenylphosphine (2 equiv), and potassium carbonate (K$_2$CO$_3$, 2 equiv) in acetonitrile (CH$_3$CN) was added and refluxed for 24 h. After the reaction was over (monitored by TLC), K$_2$CO$_3$ was filtered and rinsed with CH$_3$CN. The filtrate was evaporated using a rotary evaporator and then purified using column chromatography to obtain the target compounds **D3-T∼D12-T**.

4.2.2.1. Compound D3-T. Yield: 26.19%. White powder. *β*-Isomer; ^{1}H NMR (600 MHz, Chloroform-d) δ 7.85−7.77 (m, 9H), 7.69 (td, J = 7.8, 3.4 Hz, 6H), 5.26 (s, 1H), 4.72 (d, J = 3.5 Hz, 1H), 4.04−3.87 (m, 2H), 3.82−3.67 (m, 2H), 2.57 (qt, J = 7.4, 4.1 Hz, 1H), 2.32 (td, J = 14.0, 3.9 Hz, 1H), 1.99 (ddd, J = 14.6, 4.9, 3.0 Hz, 2H), 1.96−1.90 (m, 2H), 1.84 (ddt, J = 13.5, 6.7, 3.5 Hz, 1H), 1.73−1.48 (m, 4H), 1.44−1.38 (m, 2H), 1.36 (s, 3H), 1.19 (td, J = 11.0, 6.2 Hz, 1H), 0.92 (d, J = 6.0 Hz, 3H), 0.83 (d, J = 7.3 Hz, 3H). ^{13}C NMR (150 MHz, Chloroform-d) δ 135.13 (d, J = 3.0 Hz, Ph-C), 133.67 (d, J = 9.0 Hz, Ph-C),

130.55 (d, J = 12.0 Hz, Ph-C), 118.18 (d, J = 85.5 Hz, Ph-C), 104.11, 101.78, 87.78, 80.88, 67.06, 66.92, 52.42, 44.20, 37.35, 36.33, 34.56, 30.79, 29.68, 26.09, 24.61 (d, J = 7.5 Hz, Ph-C), 23.11 (d, J = 3.0 Hz, Ph-C), 20.34, 13.19. HRESI-MS m/z $C_{36}H_{44}O_5P^+$ 587.2939 (M-Br)$^+$.

4.2.2.2. Compound D4-T. Yield: 21.09%. White solid. $\alpha{:}\beta$ = 5:4; ^{1}H NMR (600 MHz, Chloroform-d) δ 7.88−7.75 (m, 9H), 7.72−7.66 (m, 6H), 5.31/5.24 (s, 1H), 4.66/4.44 (d, J = 3.5 Hz and J = 9.2 Hz, 1H), 4.06−3.95/ 3.94−3.88 (m, 1H), 3.82−3.74 (m, 2H), 3.61−3.53/3.37−3.33 (m, 1H), 2.79−2.59 (m, 1H), 2.53 (tdd, J = 10.0, 6.7, 3.3 Hz, 1H), 2.43−2.16 (m, 4H), 2.04− 1.93 (m, 3H), 1.79−1.65 (m, 3H), 1.58−1.44 (m, 3H), 1.40/ 1.39 (s, 3H), 1.08−1.05 (m, 1H), 0.93/0.91 (d, J = 6.0 Hz, 3H), 0.75/0.69 (d, J = 3 Hz, 3H). ^{13}C NMR (150 MHz, Chloroform-d) δ 134.97/134.92 (d, J = 3.0 Hz, Ph-C), 133.81/133.72/ 133.69 (d, J = 9.0 Hz, Ph-C), 130.48/130.46 (d, J = 12.0 Hz, Ph-C), 118.39/118.33 (d, J = 85.5 Hz, Ph-C), 104.07/103.99, 101.88/99.84, 91.20/87.80, 80.96/80.59, 67.53/66.66, 59.90/ 59.52, 52.46/51.76, 45.41/45.31, 38.15, 37.36/37.28, 36.38/ 36.27, 34.51/34.19, 32.96, 31.24/30.77, 26.16/25.70, 24.65/ 24.42, 22.69, 20.37/20.28, 13.01/12.63. HRESI-MS m/z $C_{37}H_{46}O_5P^+$ 601.3088 (M-Br)$^+$.

4.2.2.3. Compound D5-T. Yield: 43.12%. White solid. $\alpha{:}\beta$ = 1:5; ^{1}H NMR (600 MHz, Chloroform-d) δ 7.85−7.82/7.68 7.63 (m, 6H), 7.78−7.76/7.56−7.52 (m, 3H), 7.71−7.70/7.48−7.43 (m, 6H), 5.32/5.37(s, 1H), 4.67/4.88 (d, J = 3.6 Hz and 5.4 Hz, 1H), 3.91−3.76 (m, 2H), 3.75−3.60 (m, 2H), 3.43−3.17 (m, 1H), 2.61−2.50 (m, 1H), 2.37−2.07 (m, 2H), 2.02−1.96 (m, 1H), 1.94−1.79 (m, 4H), 1.72−1.65 (m, 4H), 1.61−1.56 (m, 3H), 1.39/1.40 (s, 3H), 0.93 (d, J = 6.3 Hz, 3H), 0.88−0.85 (t, J = 7.8 Hz, 2H), 0.80 (d, J = 7.3 Hz, 3H). ^{13}C NMR (150 MHz, Chloroform-d) δ 135.00 (d, J = 3.0 Hz, Ph-C), 133.77 (d, J = 9.0 Hz, Ph-C), 133.70 (d, J = 7.5 Hz, Ph-C), 132.09 (d, J = 9.0 Hz, Ph-C), 131.97, 131.96, 130.51/128.51 (d, J = 12.0 Hz, Ph-C), 118.43 (d, J = 85.5 Hz, Ph-C), 104.04, 101.98/102.15, 87.90/ 88.30, 81.12/80.53, 67.89, 59.52, 55.62/52.55, 44.41, 38.15, 37.40, 36.43, 34.60, 31.93/31.24, 30.87, 29.16, 26.19, 24.67, 24.46, 20.37, 14.12/13.09. HRESI-MS m/z $C_{38}H_{48}O_5P^+$ 615.3240 (M-Br)$^+$.

4.2.2.4. Compound D6-T. Yield: 25.52%. White solid. $\alpha{:}\beta$ = 1:1; ^{1}H NMR (600 MHz, Chloroform-d) δ 7.85 (dddd, J = 14.0, 12.5, 8.4, 1.3 Hz, 6H), 7.78 (tt, J = 7.4, 1.6 Hz, 3H), 7.70 (ddt, J = 11.0, 7.4, 3.3 Hz, 6H), 5.33/5.31 (s, 1H), 4.70/4.38 (d, J = 3.5 Hz and 9.2 Hz, 1H), 3.93−3.69 (m, 3H), 3.38−3.24 (m, 1H), 2.38−2.29 (m, 1H), 2.04−1.95 (m, 1H), 1.85 (ddt, J = 13.9, 7.0, 3.6 Hz, 1H), 1.78−1.73 (m, 2H), 1.71−1.66 (m, 3H), 1.64− 1.58 (m, 3H), 1.56−1.42 (m, 5H), 1.40/1.39 (s, 3H), 1.37−1.25 (m, 4H), 0.94/0.93 (d, J = 6.6 Hz, 3H), 0.84/0.82 (d, J = 7.2 Hz, 3H). ^{13}C NMR (150 MHz, Chloroform-d) δ 134.98/134.95 (d, J = 3.0 Hz, Ph-C), 133.75/133.69 (d, J = 9.0 Hz, Ph-C), 130.50/ 130.46 (d, J = 12.0 Hz, Ph-C), 118.50/118.43 (d, J = 85.5 Hz, Ph-C), 104.18/104.03, 101.91/100.07, 91.19/87.89, 81.16/ 80.45, 68.94/68.29, 52.58/51.70, 45.36/44.45, 38.15, 37.41/ 37.33, 36.45/36.35, 34.59/34.23, 32.74, 31.24/30.92, 29.25/ 28.90, 26.22/26.08, 25.97/25.48, 24.68/24.46, 22.21, 20.37/ 20.29, 14.13/13.87, 13.06/12.67. HRESI-MS m/z $C_{39}H_{50}O_5P^+$ 629.3397 (M-Br)$^+$.

4.2.2.5. Compound D7-T. Yield: 25.52%. White solid. $\alpha{:}\beta$ = 1:3; ^{1}H NMR (600 MHz, Chloroform-d) δ 7.87−7.75 (m, 9H), 7.70 (td, J = 7.7, 3.3 Hz, 6H), 5.34/5.31 (s, 1H), 4.71/4.38 (d, J = 3.6 Hz and 9.2 Hz, 1H), 3.90−3.65 (m, 3H), 3.36−3.24 (m, 1H), 2.38−2.27 (m, 2H), 2.24−1.93 (m, 2H), 1.84−1.82 (m, 2H), 1.77−1.65 (m, 2H), 1.54−1.43 (m, 4H), 1.40/1.39 (s,

3H), 1.33−1.13 (m, 10H), 0.94/0.93 (d, J = 6.0 Hz, 3H), 0.84/ 0.81 (d, J = 7.2 Hz, 3H). ^{13}C NMR (150 MHz, Chloroform-d) δ 135.02/134.98 (d, J = 3.0 Hz, Ph-C), 133.71/133.68 (d, J = 9.0 Hz, Ph-C), 130.51/130.48 (d, J = 12.0 Hz, Ph-C), 118.40/ 118.44 (d, J = 85.5 Hz, Ph-C), 104.21/104.04, 101.94/100.13, 91.18/87.90, 81.19/80.44, 69.14/68.38, 52.59/51.69, 45.35/ 44.48, 37.42/37.34, 36.45/36.34, 34.62/34.23, 32.71, 30.92, 30.26, 30.16, 29.54/29.35, 29.04/28.80, 26.23/26.07, 25.82/ 25.50, 24.68/24.44, 22.46/22.21, 20.39/20.29, 13.06/12.66. HRESI-MS m/z $C_{40}H_{52}O_5P^+$ 643.3559 (M-Br)$^+$.

4.2.2.6. Compound D8-T. Yield: 22.36%. White solid. $\alpha{:}\beta$ = 1:1; ^{1}H NMR (600 MHz, Chloroform-d) δ 7.87−7.76 (m, 10H), 7.72−7.67 (m, 5H), 5.35/5.31 (s, 1H), 4.72/4.38 (d, J = 3.5 and 9.3 Hz, 1H), 3.92−3.69 (m, 3H), 3.63/3.58 (t, J = 6.6 Hz, 1H), 3.38−3.26 (m, 2H), 2.64−2.29 (m, 2H), 2.03−1.96 (m, 2H), 1.94−1.80 (m, 4H), 1.80−1.65 (m, 3H), 1.56−1.44 (m, 5H), 1.41/1.40 (s, 1H), 1.34−1.27 (m, 3H), 1.21−1.13 (m, 3H), 1.07−0.95 (m, 1H), 0.94/0.93 (d, J = 6.6 Hz, 3H), 0.91− 0.87 (m, 1H), 0.86/0.84 (d, J = 7.2 Hz, 3H). ^{13}C NMR (150 MHz, Chloroform-d) δ 135.02/134.99 (d, J = 3.0 Hz, Ph-C), 133.70/133.68 (d, J = 9.0 Hz, Ph-C), 132.08 (d, J = 9.0 Hz, Ph-C), 131.97 (d, J = 3.0 Hz, Ph-C), 130.51/130.48 (d, J = 12.0 Hz, Ph-C), 128.51 (d, J = 12.0 Hz, Ph-C), 118.44/118.40 (d, J = 85.5 Hz, Ph-C), 104.21/104.03, 101.90/100.13, 91.19/87.90, 81.18/ 80.43, 69.21/68.41, 52.60/51.69, 45.35/44.48, 38.14, 37.44/ 37.35, 36.45/36.35, 34.87/34.84, 34.23, 31.92, 31.24/30.94, 29.56/29.39, 29.21/29.01, 28.95/28.84, 26.23/26.13, 26.08/ 25.79, 24.68/24.45, 22.59/22.22, 20.39/20.29, 13.06/12.66. HRESI-MS m/z $C_{41}H_{54}O_5P^+$ 657.3715 (M-Br)$^+$.

4.2.2.7. Compound D9-T. Yield: 17.71%. White solid. $\alpha{:}\beta$ = 1:4; ^{1}H NMR (600 MHz, Chloroform-d) δ 7.87 (dddd, J = 12.5, 6.7, 3.2, 1.3 Hz, 6H), 7.83−7.79 (m, 3H), 7.76−7.69 (m, 6H), 5.39/5.35 (s, 1H), 4.77/4.42 (d, J = 3.0 Hz and 9.2 Hz, 1H), 3.99−3.61 (m, 4H), 3.42−3.31 (m, 1H), 2.44−2.30 (m, 1H), 2.07−1.98 (m, 1H), 1.95−1.68 (m, 7H), 1.59−1.47 (m, 4H), 1.46−1.38 (m, 4H), 1.37−1.28 (m, 6H), 1.24−1.16 (m, 5H), 0.97/0.96 (d, J = 6.6 Hz, 3H), 0.89/0.88 (d, J = 7.2 Hz, 3H). ^{13}C NMR (150 MHz, Chloroform-d) δ 134.97 (d, J = 3.0 Hz, Ph-C), 133.73/133.71 (d, J = 10.5 Hz, Ph-C), 132.09 (d, J = 9.0 Hz, Ph-C), 131.95 (d, J = 3.0 Hz, Ph-C), 130.48/130.43 (d, J = 13.5 Hz, Ph-C), 128.54/128.51 (d, J = 12.0 Hz, Ph-C), 118.48 (d, J = 85.5 Hz, Ph-C), 104.21/104.03, 101.93/100.10, 91.20/87.91, 81.20/ 80.41, 69.23/68.45, 52.61/51.70, 45.37/44.51, 38.15, 37.44/ 37.36, 36.47/36.36, 34.24, 32.71, 31.24/30.96, 29.66, 29.45/ 29.36, 29.17, 26.08, 25.84, 24.70, 22.56, 22.27/22.23, 20.40/ 20.29, 14.13/13.84, 13.06/12.66. HRESI-MS m/z $C_{42}H_{56}O_5P^+$ 671.3870 (M-Br)$^+$.

4.2.2.8. Compound D10-T. Yield: 20.86%. White solid. $\alpha{:}\beta$ = 1:10; ^{1}H NMR (600 MHz, Chloroform-d) δ 7.87−7.75 (m, 9H), 7.70 (td, J = 7.8, 3.4 Hz, 6H), 5.36/5.31 (s, 1H), 4.74/4.39 (d, J = 3.0 Hz and 9.2 Hz, 1H), 3.94−3.56 (m, 4H), 3.41−3.28 (m, 1H), 2.41−2.28 (m, 2H), 1.92−1.81 (m, 4H), 1.79−1.66 (m, 3H), 1.56−1.43 (m, 5H), 1.41 (s, 3H), 1.34−1.25 (m, 4H), 1.22−1.12 (m, 8H), 1.02−0.95 (m, 1H), 0.94/0.93 (d, J = 6.6 Hz, 3H), 0.86/0.85 (d, J = 7.2 Hz, 3H). ^{13}C NMR (150 MHz, Chloroform-d) δ 135.03/130.54 (d, J = 3.0 Hz, Ph-C), 134.67/ 132.08 (d, J = 9.0 Hz, Ph-C), 130.52/130.49 (d, J = 10.5 Hz, Ph-C), 128.52 (d, J = 12.0 Hz, Ph-C), 118.43/118.40 (d, J = 85.5 Hz, Ph-C), 104.22/104.03, 100.14, 91.19, 80.42, 69.29, 52.60/ 51.69, 45.35, 37.36, 36.35, 34.24, 32.70/32.62, 29.51, 29.36, 29.26, 29.11, 29.02, 26.07, 25.90, 24.70, 24.45, 22.61, 22.22, 20.40, 20.29, 13.05/12.65. HRESI-MS m/z $C_{43}H_{58}O_5P^+$ 685.4022 (M-Br)$^+$.

4.2.2.9. Compound D11-T. Yield: 18.18%. White solid. $\alpha:\beta =$ 1:4; ^{1}H NMR (600 MHz, Chloroform-d) δ 7.87−7.80/7.67−7.62 (m, 6H), 7.90−7.79/7.56−7.52 (m, 3H), 7.70/7.45 (ddd, J = 11.2, 6.4, 3.4 Hz, 6H), 5.37/5.32 (s, 1H), 4.75/4.40 (d, J = 3.0 Hz and 9.2 Hz, 1H), 3.96−3.68 (m, 3H), 3.64−3.30 (m, 1H), 2.43−2.32 (m, 2H), 2.05−1.97 (m, 1H), 1.94−1.78 (m, 5H), 1.77−1.65 (m, 3H), 1.58−1.44 (m, 4H), 1.42/1.41 (s, 3H), 1.40−1.37 (m, 1H), 1.36−1.27 (m, 5H), 1.22−1.14 (m, 8H), 1.03−0.97 (m, 1H), 0.95/0.92 (d, J = 6.6 Hz, 3H), 0.86 (d, J = 7.2 Hz, 3H). ^{13}C NMR (150 MHz, Chloroform-d) δ 135.00 (d, J = 3.0 Hz, Ph-C), 133.71/133.69 (d, J = 9.0 Hz, Ph-C), 132.09 (d, J = 10.5 Hz, Ph-C), 131.97 (d, J = 3.0 Hz, Ph-C), 130.49/130.47 (d, J = 12.0 Hz, Ph-C), 128.51 (d, J = 12.0 Hz, Ph-C), 118.47/118.44 (d, J = 85.5 Hz, Ph-C), 104.22/104.03, 101.92/100.13, 91.20/87.91, 81.19/80.41, 69.30/68.46, 52.61/51.69, 45.36/44.51, 37.46/37.37, 36.46/36.35, 34.68/34.25, 31.24, 29.52/29.49, 29.41, 29.37, 29.31, 29.21, 29.15, 29.09, 26.07, 25.93, 24.71/24.46, 22.92, 22.64/22.60, 22.22, 20.40/20.29, 13.06/12.65. HRESI-MS m/z C$_{44}$H$_{60}$O$_5$P$^+$ 699.4175 (M-Br)$^+$.

4.2.2.10. Compound D12-T. Yield: 28.93%. White solid. $\alpha:\beta$ = 1:10; ^{1}H NMR (600 MHz, Chloroform-d) δ 7.83/7.65 (ddt, J = 12.5, 7.0, 1.3 Hz, 6H), 7.80−7.76/7.55−7.52 (m, 3H), 7.73−7.67/7.47−7.44 (m, 6H), 5.32/5.37 (s, 1H), 4.40/4.75 (d, J = 9.2 Hz and 3.6 Hz, 1H), 3.93 (ddd, J = 9.6, 7.1, 5.8 Hz, 1H), 3.83−3.65 (m, 2H), 3.41−3.32 (m, 1H), 2.37 (dddd, J = 17.4, 14.5, 10.2, 4.3 Hz, 2H), 2.05−1.93 (m, 1H), 1.86 (ddt, J = 13.7, 6.8, 3.5 Hz, 1H), 1.74 (dt, J = 13.6, 3.8 Hz, 2H), 1.68 (dq, J = 13.3, 3.4 Hz, 1H), 1.56−1.43 (m, 4H), 1.42−1.39 (m, 4H), 1.35−1.25 (m, 7H), 1.23−1.15 (m, 11H), 1.10 (s, 2H), 1.03−0.96 (m, 1H), 0.94 (d, J = 6.2 Hz, 3H), 0.89−0.82 (m, 3H). ^{13}C NMR (150 MHz, Chloroform-d) δ 134.98/131.96 (d, J = 3.0 Hz, Ph-C), 133.70/132.09 (d, J = 9.0 Hz, Ph-C), 130.48/130.47 (d, J = 12.0 Hz, Ph-C), 128.51 (d, J = 12.0 Hz, Ph-C), 118.42/118.41 (d, J = 85.5 Hz, Ph-C), 104.22/104.03, 101.93/100.13, 91.20, 80.40, 69.30, 51.69, 45.36, 38.15, 37.37, 36.35, 34.25, 32.69, 31.24, 30.38 (d, J = 15.0 Hz), 29.55, 29.48, 29.45, 29.37, 29.18, 29.11, 26.07, 25.97, 24.71, 22.92, 22.62 (d, J = 4.5 Hz), 22.22, 20.30, 12.65. HRESI-MS m/z C$_{45}$H$_{62}$O$_5$P$^+$ 713.4339 (M-Br)$^+$.

4.3. Biological Assays. *4.3.1. Cell Lines and Culture Conditions.* Human bladder cancer cell lines (J82 and T24) were obtained from Dr. P Guo (Xi'an Jiaotong University). The human lung cancer cell line (A549) was purchased from ATCC. The human ovarian cancer cell line (OVCAR3) was purchased from China center for type culture collection. The human ovarian cancer cell line (SKOV3) was a gift from Xiangya hospital, China. The human umbilical vein endothelial cell line (HUVEC) also was a gift from Prof. F. Y. Chen (Shanghai Jiaotong University, China). SKOV3 and OVCAR3 cells were grown in RPMI 1640 (Procell, China) supplemented with 20% fetal bovine serum (Procell, China) and 1% penicillin/streptomycin mixture. A549 and HUVEC cells were grown in DMEM (Hyclone, Logan, UT, USA) supplemented with 10% fetal bovine serum (Procell, China) and 1% penicillin/streptomycin mixture. J82 cells were grown in MEM (Procell, China) supplemented with 10% fetal bovine serum (Procell, China) and 1% penicillin/streptomycin mixture. T24 cells was grown in 5A (Procell, China) supplemented with 10% fetal bovine serum (Procell, China) and 1% penicillin/streptomycin mixture. In addition, all cells were maintained in a 37 °C, 5% CO$_2$ humidified incubator.

4.3.2. Mitochondrial Uptake Analysis. HPLC was used to detect and quantify **D8-T** and DHA. T24 cells were seeded into 10 cm culture dishes. After the cell density reached 90%, T24 cells were treated with 10 μM **D8-T** or DHA for 4 h, respectively. Then mitochondria were extracted from T24 cells according to the kit instructions (Solarbio, China). The mitochondria pellet was diluted in PBS and extracted twice with a dichloromethane/methanol mixture. After the organic layers were combined and dried, the dry residue was dissolved in chromatography acetonitrile and then used for HPLC analysis (Agilent Technologies, CA, USA). Analyses were performed on a Diamonsil-C18 column (4.6 × 250 mm, 5 μm) using acetonitrile/water as the solvent, and peaks were detected at 210 nm.

4.3.3. ATP Content Analysis. J82 and T24 cells were planted in six-well plates (2 × 10^5 cells per well). After 12 h, cells were treated with different concentrations (0, 25, 50, 100 nM) of **D8-T** for 48 h. Then, the culture medium was aspirated, and the cells were washed twice with PBS. Two hundred microliters of lysis buffer was added to each well of the six-well plate to lyse the cells. After the lysis was completed, centrifugation at 12,000g at 4 °C was performed for 5 min, and the supernatant was taken for subsequent detection. Protein concentration was quantitatively collected in each sample with a BCA protein quantification kit (Beyotime, China). 100 μL of the prepared ATP working solution was added to each well of an opaque 96-well plate and left at room temperature for 5 min to eliminate background ATP. Twenty microliters of sample or standard was added to each test well and quickly mixed with a pipette, and the RLU value was measured using a microplate reader (Biotek, SYNERGY HTX, Vermont, USA).

4.3.4. MTT Assays. The antitumor activity of **D3-T** to **D12-T** was assessed using the OVCAR3, SKOV3, J82, T24, and A549 cancer cell lines and normal HUVEC cell line via the MTT assay. The cells were cultured at a density of 5000 cells/well in a 96-well plate. Five different concentrations (0, 30, 100, 300, and 1000 nM) of **D3-T** to **D12-T** were subsequently added to the wells. Each concentration was tested in triplicate. After incubation under 5% CO$_2$ at 37 °C for 72 h, 50 μL of MTT (2 mg/mL) was added to each well, and the cells were incubated for another 4 h. Then, the liquid in each well was removed, and DMSO (150 μL) was added. The absorbance (OD values) at 490 nm was measured using a microplate reader (Biotek, SYNERGY HTX, Vermont, USA).

4.3.5. Clonogenic Assay. J82 and T24 cell lines (1.0 × 10^3 cells per well) were plated in 24-well plates. After 24 h, cells were treated with different concentrations (0, 12.5, 25, 50 nM) of **D8-T** and DHA in triplicate for 6−8 days. After washing with PBS, the cells were fixed with 10% formaldehyde solution. Finally, 0.1% crystal violet was added to each well to stain the cells. Absorbance was measured at 550 nm by using a microplate reader (Biotek, SYNERGY HTX, Vermont, USA).

4.3.6. Wound Healing Assay. Briefly, T24 and J82 cells were planted in 12-well plates (5 × 10^5 cells/well). After the density of cells reached 90%, a wound was created on the monolayer of cell by using a 200 μL pipette tip. The floating cells were washed off with PBS three times. Then, different concentrations (0, 25, 50 nM) of **D8-T** and DHA which were dissolved in serum-free medium were added. Finally, the scratch widths of 0, 12, and 24 h were recorded and imaged using a fluorescence microscope (DFC450C; Leica, Wetzlar, Germany).

4.3.7. Cell Apoptosis Determination. Cells were collected and subjected to apoptosis assay using an annexin V-fluoresceine isothiocyanate (FITC)/ PI apoptosis detection kit (Vazyme) based on the manual. In brief, J82 cells (5 × 10^5 cells/well) were

plated in six-well plates. After 12 h, cells were treated with **D8-T** (0, 800 nM) for 48 h and then washed with cold PBS three times. The cells were resuspended in binding buffer. Five microliters of annexin V-FITC conjugate and five microliters of PI solution were added. After incubation in the dark for 10 min at room temperature, flow cytometry was adopted for analysis (Becton Dickinson).

4.3.8. Measurement of Intracellular ROS Generation. The intracellular ROS accumulation was detected by flow cytometry using a ROS detection kit (Beyotime, China). J82 cells were cultured in 12-well plates (3×10^5 cells/well) for 24 h. After adding **D8-T** (0, 50, and 100 nM) for 12 h, the culture supernatants were removed, and the cells were then incubated with 10 μM DCFH-DA in fresh medium at 37 °C for 30 min. After incubation, the culture medium was removed, and the cells were washed with serum-free medium three times and then analyzed by flow cytometry.

4.3.9. JC-1 Assay. MMP was detected by the JC-1 (Solarbio, Beijing, China) staining method. Briefly, J82 cells (5.0×10^5 cells per well) were plated in six-well plates. After 12 h, cells were treated with different concentrations (0, 25, 50, and 100 nM) of **D8-T** for 48 h. After staining with JC-1 stain working solution (0.5 mL) at 37 °C for 20 min and JC-1 staining buffer ($1\times$) washing twice, the cells were resuspended using JC-1 staining buffer ($1\times$). Flow cytometry (Becton Dickinson) was used to measure MMP.

4.3.10. RNA-seq Assay. Cells were plated in six-well plates at a density of 3×10^5 cells/well in triplicate and incubated overnight for attachment. The cells were treated with or without 200 nM **D8-T** for 48 h prior to RNA isolation and RNA-seq analysis. RNA-seq analysis was outsourced to BGI Genomics (Wuhan, China), and the results were analyzed on the Dr. Tom system from BGI (https://biosys.bgi.com/).

4.3.11. EdU Assay. The EdU assay was conducted using an EdU Imaging kit (Cy5) according to the manufacturer's instructions. The results were visualized using a fluorescence microscope at a magnification of 100×, and the signals were counted in at least five random fields.

4.3.12. Cell Cycle Assay. Cells were collected and washed twice with ice-cold PBS. Then cells were fixed with 500 μL of precooled 70% ethanol at 4 °C for 6 h. Next the samples were washed twice with PBS and incubated with 500 μL of staining solution (RNase A solution, Nuclear Dye and 1× Assay Buffer in a ratio of 1:2:100) at room temperature for 30 min. Final results were analyzed by flow cytometry.

4.3.13. Western Blot Analysis. J82 and T24 cell lines were seeded (5.0×10^5 cells/well) on six-well plates. The **D8-T** was added 12 h following seeding, and cells were incubated for additional 48 h and then washed with cold-ice PBS two times, and the lysate was added for 30 min on ice. The protein extract was denatured in a 100 °C bath and analyzed on 12% SDS-PAGE gels. The gels were blotted onto the PVDF membrane and blocked with 5% milk in TBST for 1 h at room temperature. The primary antibodies used for western blot were Bax, Bcl2, cyclin D1, CDK6, CDK4, p21, and β-actin. Then, the membranes were infrared secondary antibodies. After washing with TBST three times, blots were scanned with a Chemi Doc (Bio-Rad, Hercules, CA, USA) after adding a Pierce Super Signal chemiluminescent substrate (Rockford, IL, USA). The protein levels were quantified by the gray values of the bands in the resulting images using the control group as the standard.

4.3.14. Statistical Analysis. The GraphPad Prism (version 6.01) software was used to analyze the data, and the results were expressed as the mean $\pm$ SD. The statistical significance of the data was analyzed by the unpaired *T*-test and was indicated as: *$P < 0.05$, **$P < 0.01$, ***$P < 0.001$, and ****$P < 0.0001$. ns: no significance.

■ ASSOCIATED CONTENT

🆂 Supporting Information

The Supporting Information is available free of charge at https://pubs.acs.org/doi/10.1021/acsomega.2c04562.

Scanned ^{1}H NMR, ^{13}C NMR, and HRESIMS spectra of synthesized compounds (Figures S1−S87) and HPLC chromatograms of target compounds D3-T~D12-T (Figures S88−S97) (PDF)

■ AUTHOR INFORMATION

Corresponding Authors

Lingli Mu — *Key Laboratory of Study and Discovery of Small Targeted Molecules of Hunan Province, Department of Pharmacy, School of Medicine, Hunan Normal University, Changsha, Hunan 410013, China*; Email: moulingli@sina.com

Xiaoping Yang — *Key Laboratory of Study and Discovery of Small Targeted Molecules of Hunan Province, Department of Pharmacy, School of Medicine, Hunan Normal University, Changsha, Hunan 410013, China*; ⓞ orcid.org/0000-0002-7839-7234; Email: Xiaoping.Yang@hunnu.edu.cn

Authors

Cangcang Xu — *Key Laboratory of Study and Discovery of Small Targeted Molecules of Hunan Province, Department of Pharmacy, School of Medicine, Hunan Normal University, Changsha, Hunan 410013, China*; ⓞ orcid.org/0000-0002-8086-6212

Linfan Xiao — *Key Laboratory of Study and Discovery of Small Targeted Molecules of Hunan Province, Department of Pharmacy, School of Medicine, Hunan Normal University, Changsha, Hunan 410013, China*

Peiyu Lin — *Key Laboratory of Study and Discovery of Small Targeted Molecules of Hunan Province, Department of Pharmacy, School of Medicine, Hunan Normal University, Changsha, Hunan 410013, China*

Xiyue Yang — *Key Laboratory of Study and Discovery of Small Targeted Molecules of Hunan Province, Department of Pharmacy, School of Medicine, Hunan Normal University, Changsha, Hunan 410013, China*

Xin Zou — *Key Laboratory of Study and Discovery of Small Targeted Molecules of Hunan Province, Department of Pharmacy, School of Medicine, Hunan Normal University, Changsha, Hunan 410013, China*

Complete contact information is available at:
https://pubs.acs.org/10.1021/acsomega.2c04562

Author Contributions

[†]C.X. and L.X. contributed equally.

Notes

The authors declare no competing financial interest.

■ REFERENCES

(1) Klayman, D. L. Qinghaosu (artemisinin): an antimalarial drug from China. *Science* 1985, 228, 1049−1055.

(2) Tu, Y. Artemisinin-A Gift from Traditional Chinese Medicine to the World (Nobel Lecture). *Angew. Chem., Int. Ed.* 2016, 55, 10210−10226.

(3) Li, Y.; Wu, Y. L. An over four millennium story behind qinghaosu (artemisinin)−a fantastic antimalarial drug from a traditional chinese herb. *Curr. Med. Chem.* 2003, 10, 2197−2230.

(4) Dai, X.; Zhang, X.; Chen, W.; Chen, Y.; Zhang, Q.; Mo, S.; Lu, J. Dihydroartemisinin: A Potential Natural Anticancer Drug. *Int. J. Biol. Sci.* 2021, 17, 603−622.

(5) Yuan, B.; Liao, F.; Shi, Z. Z.; Ren, Y.; Deng, X. L.; Yang, T. T.; Li, D. Y.; Li, R. F.; Pu, D. D.; Wang, Y. J.; et al. Dihydroartemisinin Inhibits the Proliferation, Colony Formation and Induces Ferroptosis of Lung Cancer Cells by Inhibiting PRIM2/SLC7A11 Axis. *OncoTargets Ther.* 2020, 13, 10829−10840.

(6) Cai, X.; Miao, J.; Sun, R.; Wang, S.; Molina-Vila, M. A.; Chaib, I.; Rosell, R.; Cao, P. Dihydroartemisinin overcomes the resistance to osimertinib in EGFR-mutant non-small-cell lung cancer. *Pharmacol. Res.* 2021, 170, No. 105701.

(7) Zheng, J.; Li, X.; Yang, W.; Zhang, F. Dihydroartemisinin regulates apoptosis, migration, and invasion of ovarian cancer cells via mediating RECK. *J. Pharmacol. Sci.* 2021, 146, 71−81.

(8) Paccez, J. D.; Duncan, K.; Sekar, D.; Correa, R. G.; Wang, Y.; Gu, X.; Bashin, M.; Chibale, K.; Libermann, T. A.; Zerbini, L. F. Dihydroartemisinin inhibits prostate cancer via JARID2/miR-7/miR-34a-dependent downregulation of Axl. *Oncogenesis* 2019, 8, 14.

(9) Wang, T.; Luo, R.; Li, W.; Yan, H.; Xie, S.; Xiao, W.; Wang, Y.; Chen, B.; Bai, P.; Xing, J. Dihydroartemisinin suppresses bladder cancer cell invasion and migration by regulating KDM3A and p21. *J. Cancer* 2020, 11, 1115−1124.

(10) Zhang, B.; Chen, X.; Gan, Y.; Li, B. S.; Wang, K. N.; He, Y. Dihydroartemisinin attenuates benign prostatic hyperplasia in rats by inhibiting prostatic epithelial cell proliferation. *Ann. Transl. Med.* 2021, 9, 1246.

(11) Zhang, Q.; Yi, H.; Yao, H.; Lu, L.; He, G.; Wu, M.; Zheng, C.; Li, Y.; Chen, S.; Li, L.; et al. Artemisinin Derivatives Inhibit Non-small Cell Lung Cancer Cells Through Induction of ROS-dependent Apoptosis/Ferroptosis. *J. Cancer* 2021, 12, 4075−4085.

(12) Wu, X.; Liu, Y.; Zhang, E.; Chen, J.; Huang, X.; Yan, H.; Cao, W.; Qu, J.; Gu, H.; Xu, R.; et al. Dihydroartemisinin Modulates Apoptosis and Autophagy in Multiple Myeloma through the P38/MAPK and Wnt/β-Catenin Signaling Pathways. *Oxid. Med. Cell. Longevity* 2020, 2020, No. 6096391.

(13) Xu, C. C.; Deng, T.; Fan, M. L.; Lv, W. B.; Liu, J. H.; Yu, B. Y. Synthesis and in vitro antitumor evaluation of dihydroartemisinin-cinnamic acid ester derivatives. *Eur. J. Med. Chem.* 2016, 107, 192−203.

(14) Xiao, L.; Xu, C.; Lin, P.; Mu, L.; Yang, X. Novel dihydroartemisinin derivative Mito-DHA(5) induces apoptosis associated with mitochondrial pathway in bladder cancer cells. *BMC Pharmacol. Toxicol.* 2022, 23, 10.

(15) Xu, C.; Xiao, L.; Zhang, X.; Zhuang, T.; Mu, L.; Yang, X. Synthesis and biological activities of novel mitochondria-targeted artemisinin ester derivatives. *Bioorg. Med. Chem. Lett.* 2021, 39, No. 127912.

(16) Nontprasert, A.; Pukrittayakamee, S.; Prakongpan, S.; Supanaranond, W.; Looareesuwan, S.; White, N. J. Assessment of the neurotoxicity of oral dihydroartemisinin in mice. *Trans. R. Soc. Trop. Med. Hyg.* 2002, 96, 99−101.

(17) Raghavamenon, A. C.; Muyiwa, A. F.; Davis, L. K.; Uppu, R. M. Dihydroartemisinin induces caspase-8-dependent apoptosis in murine GT1-7 hypothalamic neurons. *Toxicol. Mech. Methods* 2011, 21, 367−373.

(18) Zong, W. X.; Rabinowitz, J. D.; White, E. Mitochondria and Cancer. *Mol. Cell* 2016, 61, 667−676.

(19) Porporato, P. E.; Filigheddu, N.; Pedro, J. M. B.; Kroemer, G.; Galluzzi, L. Mitochondrial metabolism and cancer. *Cell Res.* 2018, 28, 265−280.

(20) Rajaputra, P.; Nkepang, G.; Watley, R.; You, Y. J. Synthesis and in vitro biological evaluation of lipophilic cation conjugated photosensitizers for targeting mitochondria. *Bioorg. Med. Chem.* 2013, 21, 379−387.

(21) Dubinin, M. V.; Semenova, A. A.; Ilzorkina, A. I.; Penkov, N. V.; Nedopekina, D. A.; Sharapov, V. A.; Khoroshavina, E. I.; Davletshin, E. V.; Belosludtseva, N. V.; Spivak, A. Y.; et al. Mitochondria-targeted prooxidant effects of betulinic acid conjugated with delocalized lipophilic cation F16. *Free Radical Biol. Med.* 2021, 168, 55−69.

(22) Shi, M. H.; Zhang, J. L.; Li, X. W.; Pan, S.; Li, J.; Yang, C. R.; Hu, H. Y.; Qiao, M. X.; Chen, D. W.; Zhao, X. L. Mitochondria-targeted delivery of doxorubicin to enhance antitumor activity with HER-2 peptide-mediated multifunctional pH-sensitive DQAsomes. *Int. J. Nanomed.* 2018, 13, 4209−4226.

(23) Fu, S. N.; Xie, Y. Q.; Tuo, J.; Wang, Y. L.; Zhu, W. B.; Wu, S. H.; Yan, G. M.; Hu, H. Y. Discovery of mitochondria-targeting berberine derivatives as the inhibitors of proliferation, invasion and migration against rat C6 and human U87 glioma cells. *MedChemComm* 2015, 6, 164−173.

(24) Shi, L.; Gao, L. L.; Cai, S. Z.; Xiong, Q. W.; Ma, Z. R. A novel selective mitochondrial-targeted curcumin analog with remarkable cytotoxicity in glioma cells. *Eur. J. Med. Chem.* 2021, 221, No. 113528.

(25) Jin, L.; Dai, L.; Ji, M.; Wang, H. Mitochondria-targeted triphenylphosphonium conjugated glycyrrhetinic acid derivatives as potent anticancer drugs. *Bioorg. Chem.* 2019, 85, 179−190.

(26) Ye, Y.; Zhang, T.; Yuan, H.; Li, D.; Lou, H.; Fan, P. Mitochondria-Targeted Lupane Triterpenoid Derivatives and Their Selective Apoptosis-Inducing Anticancer Mechanisms. *J. Med. Chem.* 2017, 60, 6353−6363.

(27) Zhang, C.; Fortin, P. Y.; Barnoin, G.; Qin, X.; Wang, X.; Fernandez Alvarez, A.; Bijani, C.; Maddelein, M. L.; Hemmert, C.; Cuvillier, O.; et al. An Artemisinin-Derivative-(NHC)Gold(I) Hybrid with Enhanced Cytotoxicity through Inhibition of NRF2 Transcriptional Activity. *Angew. Chem., Int. Ed.* 2020, 59, 12062−12068.

(28) Wu, J. M.; Shan, F.; Wu, G. S.; Li, Y.; Ding, J.; Xiao, D.; Han, J. X.; Atassi, G.; Leonce, S.; Caignard, D. H.; et al. Synthesis and cytotoxicity of artemisinin derivatives containing cyanoarylmethyl group. *Eur. J. Med. Chem.* 2001, 36, 469−479.

(29) Smit, F. J.; van Biljon, R. A.; Birkholtz, L.-M.; N'Da, D. D. Synthesis and in vitro biological evaluation of dihydroartemisinyl-chalcone esters. *Eur. J. Med. Chem.* 2015, 90, 33−44.

(30) Burke, P. J. Mitochondria, Bioenergetics and Apoptosis in Cancer. *Trends Cancer* 2017, 3, 857−870.

(31) Dietrich, D. R. Toxicological and pathological applications of proliferating cell nuclear antigen (PCNA), a novel endogenous marker for cell proliferation. *Crit. Rev. Toxicol.* 1993, 23, 77−109.

(32) Salazar-Roa, M.; Malumbres, M. Fueling the Cell Division Cycle. *Trends Cell Biol.* 2017, 27, 69−81.

(33) Schatton, D.; Di Pietro, G.; Szczepanowska, K.; Veronese, M.; Marx, M. C.; Braunöhler, K.; Barth, E.; Müller, S.; Giavalisco, P.; Langer, T.; et al. CLUH controls astrin-1 expression to couple mitochondrial metabolism to cell cycle progression. *eLife* 2022, 11, No. e74552.

(34) Scodelaro Bilbao, P.; Boland, R. Extracellular ATP regulates FoxO family of transcription factors and cell cycle progression through PI3K/Akt in MCF-7 cells. *Biochim. Biophys. Acta* 2013, 1830, 4456−4469.

(35) Sholl-Franco, A.; Fragel-Madeira, L.; Macama Ada, C.; Linden, R.; Ventura, A. L. ATP controls cell cycle and induces proliferation in the mouse developing retina. *Int. J. Dev. Neurosci.* **2010**, *28*, 63−73.

(36) Kasten, M. M; Giordano, A. pRb and the cdks in apoptosis and the cell cycle. *Cell Death Differ.* **1998**, *5*, 132−140.